

---

# Deep Statistical Arbitrage: Name Space versus Rank Space

---

**Anonymous Author(s)**

Affiliation

Address

email

## Abstract

1      Equity market dynamics are conventionally investigated in name space, where  
2 stocks are indexed by company names. However, this perspective often suffers  
3 from high volatility and a low signal-to-noise ratio, which poses challenges for  
4 effective learning by deep neural networks (DNNs). In contrast, by indexing  
5 stocks by their ranks in capitalization, we gain a distinct and more structured  
6 view of market behavior in rank space. In this work, we demonstrate that DNNs  
7 achieve superior performance in statistical arbitrage when operating in rank space  
8 compared to name space. This performance gain is driven by more robust market  
9 representations and enhanced mean-reverting properties of residual returns in  
10 rank space, which facilitate more efficient learning. Our findings highlight the  
11 critical role of domain-informed data transformation in improving deep learning  
12 performance in noisy financial environments.

13 **1 Introduction**

14 In equity markets, stocks are conventionally labeled by fixed company identifiers (company names),  
15 a perspective that often suffers from high volatility and a low signal-to-noise ratio, hindering effective  
16 learning by deep neural networks (DNNs).

17 As an alternative, we consider a rank-space representation, where stocks are indexed by their ranks in  
18 capitalization rather than fixed company identifiers. In this view, we focus on the stock at a given  
19 rank in capitalization while the corresponding company name may change. This formulation offers a  
20 more structured and stable view of market dynamics. We refer to a market labeled by fixed company  
21 identifiers (company names) as the *market in name space*, and one labeled by ranks in capitalization  
22 as the *market in rank space*.

23 A structured market dynamics is crucial for the performance of statistical arbitrage, a **market-neutral**  
24 **strategy that seeks to exploit temporary mispricing among related assets**[3, 14]. Specifically, it  
25 constructs portfolios that rely on the residual returns, the component of returns unexplained by market  
26 factors, and profits if these residuals exhibit mean-reverting behavior. Therefore, the presence of  
27 **structured market dynamics, particularly mean reversion in residuals, is crucial to its performance.**

28 In this paper, we show that operating statistical arbitrage in rank space by DNNs significantly  
29 outperforms the name-space counterpart. Our DNN-based rank-space portfolios achieve an average  
30 annual return 35.68% and an average Sharpe ratio of 3.28 from 2007 to 2022, accounting for a  
31 2-basis-point transaction cost. In contrast, applying the same DNNs in name space yields negligible  
32 returns over the same period.

33 Further comparison shows that DNN-based rank-space portfolios not only exploit the importance of  
34 mean-reversion during mean-variance optimization, but also implement more intelligent strategies  
35 than traditional parametric model by applying flexible leverage and minimizing carry risk. We

36 attribute these improvements to two key advantages of rank space: (i) a more robust and stable  
 37 representation of market structure, and (ii) enhanced mean-reverting behavior in residual returns.  
 38 Together, these properties enable DNNs to extract actionable signals from noisy financial data.  
 39 Our findings highlight the importance of domain-informed data representations in financial machine  
 40 learning. In particular, they show how appropriate input transformation can significantly improve  
 41 the learning efficiency and performance of deep models in complex, noisy environments like equity  
 42 markets[9, 23].  
 43 The remainder of the paper is organized as follows. Section 2 reviews related work. Section 3  
 44 formulates the framework for statistical arbitrage in both name space and rank space. Section 4  
 45 presents our empirical results using U.S. equity data. Section 5 concludes with a discussion of  
 46 implications and future directions.

## 47 2 Related work

48 Our results add to the burgeoning literature on machine learning applications in finance. Gu *et al.*  
 49 systematically compare various machine learning methods for predicting stock returns[13]. Aceri *et al.*  
 50 utilize deep reinforcement learning for portfolio managements[1]. Araci explores the correlation  
 51 between financial news and stock returns by BERT language model[2]. Horvath *et al.* apply deep  
 52 neural networks to calibrate volatility surface in fixed-income markets[17].  
 53 Our research advances the understanding of statistical arbitrage. While this problem can be framed as a  
 54 stochastic control problem solvable via the Hamilton-Jacobi-Bellman (HJB) equation[10, 20, 25, 29],  
 55 practical applications are often limited by calibration challenges and the absence of selection mecha-  
 56 nism in diverse markets. To address these issues, Avellaneda and Lee[3] propose a pragmatic trading  
 57 strategy based on Ornstein–Uhlenbeck (OU) processes, later refined by Yeo and Papanicolaou[28].  
 58 More recently, Mulvey *et al.*[22] combine the HJB framework with feed-forward networks, while Kim  
 59 *et al.*[19] apply deep reinforcement learning to optimize pair trading strategies. Guijarro-Ordonez *et*  
 60 *al.*[14] provide a comprehensive survey of deep learning models for statistical arbitrage.  
 61 Our paper also enriches the emerging literature on rank-based market models. Fernholz *et al.*, in  
 62 their seminal work on stochastic portfolio theory, introduce the concept of functionally generated  
 63 portfolios in both name and rank spaces[11]. Building on this foundation, Banner *et al.*[7] and Ichiba  
 64 *et al.*[18] study the dynamics of rank capitalizations and gap processes in hybrid Atlas models, starkly  
 65 contrasting the dynamics in name space. Healy *et al.*[16] demonstrate that rank space exhibits a more  
 66 structured market in rank space, theoretically establishing a larger spectral gap in the correlation  
 67 matrix compared to name space, supported by comprehensive empirical validation (Figure 3). These  
 68 theoretical insights form the basis for our proposed statistical arbitrage strategy in rank space.

## 69 3 Formulation

70 This section formulates statistical arbitrage in name and rank space. A schematic overview is shown in  
 71 Fig. 1. Supplementary implementation details in Appendix A, with detailed algorithmic pseudocode  
 72 is provided in Appendix A.4. The code is available at [https://github.com/Infi-Yingfei-Li/  
 73 stats-arb-rank-space](https://github.com/Infi-Yingfei-Li/stats-arb-rank-space).

### 74 3.1 Market decomposition

#### 75 3.1.1 Name space

76 In a market consisting of  $N$  stocks, we denote the dividend-adjusted return<sup>1</sup> on stock  $i$  at trading day  
 77  $t$  by  $r_{i,t}$ . We adopt a standard factor model for stock returns,

$$r_t - r_f = \beta_t F_t + \epsilon_t, \quad t = 1, 2, \dots, T. \quad (3.1)$$

78 Here,  $r_t = \{r_{i,t}\}_{i=1}^N \in \mathbb{R}^N$  are the dividend-adjusted daily return,  $r_f \in \mathbb{R}$  is the risk-free rate<sup>2</sup>,  
 79  $F_t \in \mathbb{R}^{K \times 1}$  are the underlying factors,  $\beta_t \in \mathbb{R}^{N \times K}$  are the corresponding loadings on  $K$  factors,  
 80 and  $\epsilon_t \in \mathbb{R}^N$  are the residual returns.

---

<sup>1</sup>The daily return of a stock that accounts for both price changes and dividend payments.

<sup>2</sup>The investment return with zero-risk financial loss, chosen as the rate of 1-month U.S. treasury bill here.

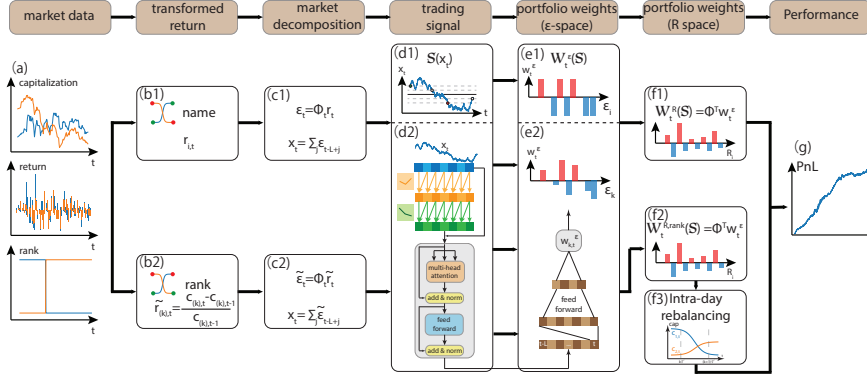


Figure 1: Schematic of the statistical arbitrage algorithm in name space and rank space.

81 Without loss of generality, these factors can be written as portfolios of stocks,

$$F_t = \omega_t(r_t - r_f), \quad (3.2)$$

82 where  $\omega_t \in \mathbb{R}^{K \times N}$  specifies the factor portfolio weights. Combining (3.1) and (3.2) yields

$$r_t - r_f = \beta_t \omega_t(r_t - r_f) + \epsilon_t \Rightarrow \epsilon_t = (I - \beta_t \omega_t)(r_t - r_f) := \Phi_t(r_t - r_f) \quad (3.3)$$

83 where  $\Phi_t := (I - \beta_t \omega_t)$  defines a linear transformation from returns to residual returns. Each  $\epsilon_{i,t}$   
84 can thus be interpreted as the return of a tradable portfolio with weights given by the  $i$ -th row of  $\Phi_t$ .

85 Consequently, we refer to the space spanned by  $r_t$  as the *name equity space*, and the space spanned  
86 by  $\epsilon_t$  as the *name residual space*. We denote the portfolio weights in name equity space as  $w_t^{R,\text{name}}$   
87 and portfolio weights in name residual space as  $w_t^{\epsilon,\text{name}}$ . These are related by

$$w_t^{R,\text{name}} = \Phi_t^T w_t^{\epsilon,\text{name}} \quad (3.4)$$

88 Importantly, given any  $w_t^{\epsilon,\text{name}}$ , the derived  $w_t^{R,\text{name}}$  are market neural (proofs in the Appendix C).

### 89 3.1.2 Rank space

90 We begin by introducing the key variables that characterize the market dynamics in rank space: the  
91 daily return on rank  $k$  at day  $t$  in the continuous-time limit, defined as

$$\tilde{r}_{(k),t} := \frac{c_{(k),t} - c_{(k),t-1}}{c_{(k),t-1}} = \frac{c_{\mathcal{I}_{(k),t},t} - c_{\mathcal{I}_{(k),t-1},t-1}}{c_{\mathcal{I}_{(k),t-1},t-1}}, \quad (3.5)$$

92 where  $c_{i,t}$  is the capitalization of stock  $i$  at day  $t$ ,  $c_{(k),t}$  is the capitalization of the stock occupying  
93 the  $k$ -th rank in descending order at day  $t$ .  $\mathcal{I}_{(k),t}$  represents the company occupying the rank  $k$  at day  
94  $t$ , and conversely,  $\mathcal{R}_{i,t}$  gives the capitalization rank of stock  $i$ . Our definition of return in rank space  
95 is motivated by the log capitalization process in the hybrid-Atlas model in Appendix B[7, 18].

96 Importantly,  $\tilde{r}_t$  does not necessarily correspond to direct financial quantity, as  $\mathcal{I}_{(k),t}$  and  $\mathcal{I}_{(k),t-1}$  may  
97 differ – meaning the stock occupying rank  $k$  can change between days. To realize  $\tilde{r}_t$  in practice, we  
98 develop an intra-day rebalancing strategy, detailed in Appendix D.

99 Following the construction in name space, we assume a factor model for  $\tilde{r}_t$ ,

$$\tilde{r}_t - r_f = \tilde{\beta}_t \tilde{F}_t + \tilde{\epsilon}_t, \quad (3.6)$$

100 where  $\tilde{r}_t = \{\tilde{r}_{(k),t}\}_{k=1}^N \in \mathbb{R}^N$ ,  $\tilde{\beta}_t \in \mathbb{R}^{N \times K}$ ,  $\tilde{F}_t \in \mathbb{R}^{K \times 1}$ , and  $\tilde{\epsilon}_t \in \mathbb{R}^N$ . Analogously, we model the  
101 factors as portfolios of rank returns

$$\tilde{r}_t - r_f = \tilde{\beta}_t \tilde{\omega}_t(\tilde{r}_t - r_f) + \tilde{\epsilon}_t \Rightarrow \tilde{\epsilon}_t = (I - \tilde{\beta}_t \tilde{\omega}_t)(\tilde{r}_t - r_f) := \tilde{\Phi}_t(\tilde{r}_t - r_f), \quad (3.7)$$

102 where  $\tilde{\Phi}_t := (I - \tilde{\beta}_t \tilde{\omega}_t)$ .

103 We refer to the space spanned by  $\tilde{r}_t$  as *rank equity space* and the space spanned by  $\tilde{\epsilon}_t$  as *rank residual  
104 space*, mirroring our definition in the name space. Let  $w_t^{R,\text{rank}}$  and  $w_t^{\epsilon,\text{rank}}$  denote the portfolio weights  
105 in rank equity space and rank residual space, respectively, related by

$$w_t^{R,\text{rank}} = \tilde{\Phi}_t^T w_t^{\epsilon,\text{rank}}, \quad (3.8)$$

106 As in name space, any  $w_t^{\epsilon,\text{rank}}$  generates a market-neutral portfolio  $w_t^{R,\text{rank}}$  (proof in Appendix C).

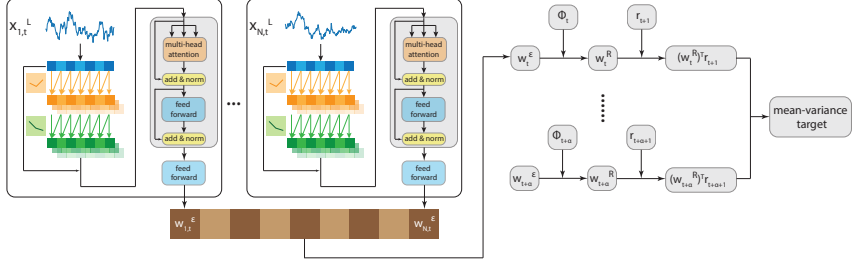


Figure 2: Schematic for the architecture of deep neural networks in both name and rank space.

### 107 3.2 Trading signals and portfolio weights

108 After computing the residual returns  $\epsilon_t$ <sup>3</sup>, we derive the cumulative residual returns over a look-back  
109 window of length  $L$ :

$$110 \quad x_t^L = (x_{t-L+1}, x_{t-L+2}, \dots, x_t), \quad (3.9)$$

111 where  $x_{t-L+\alpha} = \sum_{j=1}^{\alpha} \epsilon_{t-L+j}$ ,  $\alpha = 1, 2, \dots, L$ .

112 We adopt DNNs  $\mathcal{N} : x_t^L \rightarrow w_t^{\epsilon|\text{NN, name/rank}}$  as a data-driven method to calculate portfolio weights in  
113 residual space  $w_t^{\epsilon}$  for both name space and rank spaces. The DNNs consist of convolutional layers to  
114 capture local patterns, followed by transformer encoder layers to model global dependencies. The  
neural networks are trained via mean-variance optimization,

$$\begin{aligned} \text{Maximize}_{\mathcal{N}(\cdot)} \quad & \mathbb{E}[(w_t^{R|\text{NN, name/rank}})^T (r_{t+1} - r_f)] - \gamma \text{Var}[(w_t^{R|\text{NN, name}})^T (r_{t+1} - r_f)] \\ \text{s.t.} \quad & w_t^{R|\text{NN, name/rank}} = \frac{\Phi_t^T w_t^{\epsilon|\text{NN, name/rank}}}{\|\Phi_t^T w_t^{\epsilon|\text{NN, name/rank}}\|_1} \\ & w_t^{\epsilon|\text{NN, name/rank}} = \mathcal{N}(x_t^L), \end{aligned} \quad (3.10)$$

115 where  $\gamma$  is the risk-aversion factor. We show a schematic for our DNNs architecture in Fig. 2 with  
116 [architecture](#) and implementation details in Appendix A.3.

117 For comparison, we benchmark the DNN performance against a classical parametric model based  
118 on Ornstein-Uhlenbeck (OU) process[3, 28], with [the model formulation](#) and execution details in  
119 Appendix E.

### 120 3.3 Intraday rebalancing

121 The portfolio weights calculated in the rank space are assigned to artificial financial instruments  
122 that yield rank returns in continuous-time limits defined in (3.5). To make the constructed portfolio  
123 practically implementable, it is necessary to convert these portfolio weights into stock-based portfolios  
124 in name space. To address the issue, we propose an intraday rebalancing mechanism.

125 Formally, given the predetermined portfolio weights in rank equity space  $\{w_{(k),t}^{\text{rank}}\}_{k=1}^N$  before the  
126 market opening, our goal is to rebalance the portfolio at fixed time intervals of  $\mathcal{T}$  minutes such that  
127 the portfolio becomes  $\{w_{(k),t}^{\text{rank}} (1 + \tilde{r}_{(k),t+1})\}_{k=1}^N$  by market close, at the sacrifice of additional costs.  
128 To facilitate this discussion, we introduce two processes:

129 **(i)**  $w_{(k),t+\tau}^{\text{rank}}$ : the dollar-valued portfolio weight for rank  $k$  at time  $t + \tau$ ;

130 **(ii)**  $w_{i,t+\tau}^{\text{name}}$ : the dollar-valued portfolio weight for stock  $i$  at time  $t + \tau$ .

131 Here,  $t$  denotes the daily time tick and  $\tau$  represents the intraday time tick. For instance, for  $t = \text{Jan, 3rd, 2022}$  (end of the day) and  $\tau = 45$  minutes,  $t + \tau$  refers to Jan, 4th, 2022 00:45 AM, and  $t + 1$   
132 refers to the end of the day on Jan, 4th, 2022.

<sup>3</sup>For simplicity, we take a unified notation  $\epsilon_t$  to denote the residual returns in both name and rank space in the following discussions unless otherwise specified.

134  $w_{(k),t+\tau}^{\text{rank}}$  is the portfolio weight on the  $k$ -th rank that evolves strictly based on the rank returns in  
 135 continuous-time limit,

$$w_{(k),t+\tau}^{\text{rank}} = w_{(k),t}^{\text{rank}}(1 + \tilde{r}_{(k),t+\tau}), \quad (3.11)$$

136 where  $\tilde{r}_{(k),t+\tau} = \frac{c_{(k),t+\tau}}{c_{(k),t}} - 1$ . Here,  $c_{(k),t+\tau}$  denotes the capitalization at  $k$ -th rank at time  $t + \tau$ .

137 In contrast,  $w_{i,t+\tau}^{\text{name}}$  is the portfolio weight on the  $i$ -th stock, evolving according to the following rules:

138 **(i)** Between the rebalancing interval when  $t + j\mathcal{T} < t + \tau \leq t + (j+1)\mathcal{T}, j \in \mathbb{N}$ ,

$$w_{i,t+\tau}^{\text{name}} = w_{i,t+(j\mathcal{T})^+}^{\text{name}} \times \frac{c_{i,t+(j\mathcal{T})^+}}{c_{i,t+(j\mathcal{T})^+}}, \quad (3.12)$$

139 where  $(j\mathcal{T})^+ := \lim_{\delta \downarrow 0} (j\mathcal{T} + \delta)$ .

140 **(ii)** At the re-balancing points when  $\tau = ((j+1)\mathcal{T})^+, j \in \mathbb{N}$ , adjust the portfolio weights via active  
 141 trading such that

$$w_{i,t+((j+1)\mathcal{T})^+}^{\text{name}} = \sum_{k=1}^n w_{(k),t+(j+1)\mathcal{T}}^{\text{rank}} \mathbf{1}_{\{\mathcal{R}_{i,t+(j+1)\mathcal{T}}=k\}}. \quad (3.13)$$

142 In other words, we carry out the conversion of portfolio weights between name space and rank space  
 143 at the rebalancing points  $\tau = ((j+1)\mathcal{T})^+, j \in \mathbb{N}$  through active trading. Notably, the value on the  
 144 trading book before trading at  $t + (j+1)\mathcal{T}$  is  $\sum_{k=1}^N w_{i,t+(j+1)\mathcal{T}}^{\text{name}}$ , while the desired value immediately  
 145 after trading is  $\sum_{i=1}^N w_{i,t+(j+1)\mathcal{T}}^{\text{name}} = \sum_{k=1}^N w_{(k),t+(j+1)\mathcal{T}}^{\text{rank}}$ . The two values are not necessarily equal  
 146 when there exists switching of ranks in capitalization between  $t + j\mathcal{T}$  and  $t + (j+1)\mathcal{T}$  (elaborated  
 147 by a case study in Appendix D and by the hybrid-Atlas model in Appendix B). Consequently, the  
 148 cost of the active trading at  $t + (j+1)\mathcal{T}$  involves two components,

$$\begin{aligned} \text{cost}(t + (j+1)\mathcal{T}^+; w_{(k),t}^{\text{rank}}) = & \left( \sum_{i=1}^N w_{i,t+(j+1)\mathcal{T}^+}^{\text{name}} - \sum_{k=1}^N w_{(k),t+(j+1)\mathcal{T}}^{\text{rank}} \right) \\ & + \eta \sum_{i=1}^N |w_{i,t+(j+1)\mathcal{T}^+}^{\text{name}} - w_{i,t+(j+1)\mathcal{T}}^{\text{name}}|, \end{aligned} \quad (3.14)$$

149 where  $\eta$  is the transaction cost factor. Here, the cost at time  $t + (j+1)\mathcal{T}^+$  depends on the portfolio  
 150 weights assigned at the beginning of the trading day,  $w_{(k),t}^{\text{rank}}$ , because the intraday portfolio weights  
 151  $w_{i,t+\tau}^{\text{name}}$  and  $w_{(k),t+\tau}^{\text{rank}}$  are recursively governed by the system dynamics ((3.11), (3.12), and (3.13))  
 152 from the initial condition  $w_{(k),t}^{\text{rank}}$ . We highlight this dependence by including the  $w_{(k),t}^{\text{rank}}$  as a parameter  
 153 for the cost in (3.14). We refer to the first term in (3.14) as latency cost, the second term as cost  
 154 from the bid-ask spread, with their sum representing the total transaction cost. The terminology are  
 155 rationalized in the case study in Appendix D.

156 The precise implementation of the intraday rebalancing is summarized in Appendix D Algorithm  
 157 4 along with a schematic in panel (f3) in Fig. 1. For our backtesting, we primarily use  $\eta = 2$  basis  
 158 points to account for the cost from the bid-ask spread. This setting approximately corresponds to a  
 159 5-10 cents bid-ask spread for our investment universe, the top 500 stocks in the U.S. equity market.

### 160 3.4 Backtesting

161 We evaluate the portfolio performance by calculating the historical profit-and-loss (PnL)  $V_t$  and the  
 162 Sharpe ratio.

163 For portfolios in name space,

$$V_{t+1} = (1 + r_{f,t+1}) \times (V_t - \sum_i \Lambda w_{i,t} V_t - \text{TC}) + \sum_i \Lambda V_t w_{i,t} (1 + r_{i,t+1}), \quad (3.15)$$

164 where  $\Lambda = 1$  is the leverage,  $r_{f,t+1}$  is the risk-free rate during the trading day  $t + 1$ , and  $w_t$  are  
 165 normalized by  $l_1$  norm. The transaction cost is given by  $\text{TC} = \eta \sum_i \Lambda |V_t w_{i,t} - V_{t-1} w_{i,t-1} (1 + r_{i,t})|$ ,  
 166 where  $\eta$  is the transaction cost factor, set to 2 basis points.

167 For portfolios in rank space, the PnL evolves as

$$V_{t+1} = (V_t - \sum_{k=1}^N w_{(k),t}^{R,\text{rank}})(1 + r_{f,t+1}) + \sum_{k=1}^N \Lambda V_t w_{(k),t}^{R,\text{rank}}(1 + \tilde{r}_{(k),t+1}) - \sum_{j:t < t+j\mathcal{T} \leq t+1} \text{cost}(t + j\mathcal{T}^+; \Lambda V_t w_{(k),t}^{R,\text{rank}}), \quad (3.16)$$

168 where the last term accounts for the transaction costs due to intraday rebalancing defined in  
169 (3.14), where we substitute generic portfolio weights  $w_{(k),t}^{\text{rank}}$  in (3.14) into specific portfolio weights  
170  $\Lambda V_t w_{(k),t}^{R,\text{rank}}$  in (3.16).

## 171 4 Empirical results for the U.S. equities

### 172 4.1 Market structure: name space versus rank space

173 We begin by comparing the market dynamics in name space and rank space, highlighting two key  
174 advantages of rank space: (i) a more structured market dynamics in rank space, and (ii) a more  
175 enhanced mean-reverting behavior of residual returns in rank space – both critical motivations for  
176 operating statistical arbitrage in rank space.

177 First, we show the market capitalization across ranks, averaged over five-year window from 1991  
178 to 2022 in Fig. 3(a), revealing a stable distribution in rank space[11]. A principal component  
179 analysis (PCA) on the correlation matrix suggests significantly larger leading eigenvalue in rank space  
180 compared to that in name space (Fig. 3(b)), implying that a greater proportion of market variance is  
181 captured by the first eigenvector in rank space. This points to a more structured and concentrated  
182 market dynamic in rank space.

183 More importantly, the single-factor structure in rank space substantially simplifies market decom-  
184 position. We present the empirical eigenvalue spectra of the correlation matrix in both spaces  
185 across different periods in Fig. 3(c1-c6) and (d1-d6). In name space, several eigenvalues exceed  
186 the Marchenko–Pastur upper bound [4], indicating a multi-factor market and consequently low  
187 signal-to-noise ratio(Fig. 3(c1-c6)). In contrast, rank space exhibits a sharp bulk-edge separation with  
188 a dominant single factor (Fig. 3(d1-d6)). This clearer structure enables more well-defined separation  
189 of market factors from residuals during market decomposition.

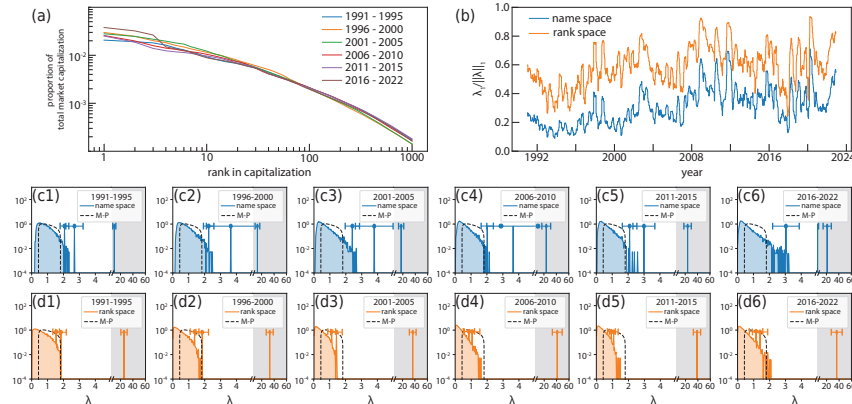
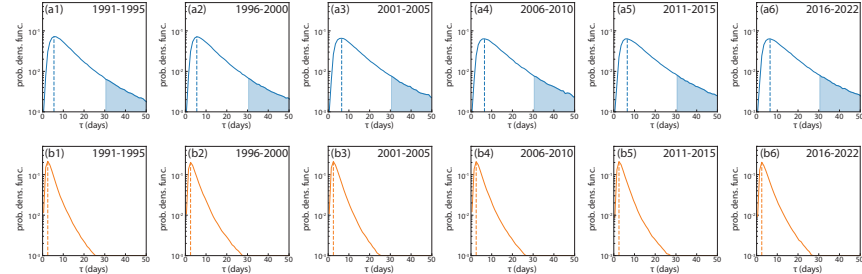


Figure 3: **Market structure in name space versus rank space.** (a) Proportion of total market capitalization versus ranks in capitalization. (b) The principal eigenvalue of the correlation matrices of  $r_t$  in name space (blue) and for  $\tilde{r}_t$  rank space (orange). (c, d) The empirical probability distribution density of the eigenvalue spectrum of the correlation matrices versus Marchenko-Pastur distribution. The market exhibits a more structured correlation in rank space compared to name space.

190 Second, we observe markedly faster mean-reversion of residual returns in rank space, critical for  
191 statistical arbitrage. We quantify mean-reversion by fitting cumulative residual returns  $x_t^L$  to an OU

process and extracting the mean-reversion time  $\tau$ . Fig. 4 shows the empirical distribution of  $\tau$  over five-year windows from 1991 to 2022. In name space (Fig. 4(a1–a6)), the distribution is heavy-tailed toward large  $\tau$ , reflecting slower mean reversion. In contrast, rank space (Fig. 4(b1–b6)) exhibits a sharper concentration in the fast mean-reverting regime, with fewer instances of slow mean-reversion ( $\tau > 30$  days, shaded area). A non-parametric analysis in Appendix F yields consistent results.



**Figure 4: Mean-reverting time  $\tau$  in name space versus rank space.** The  $\tau$  is evaluated by fitting the cumulative residual return  $x_t^L$  to an Ornstein–Uhlenbeck(OU) process. **(a1-a6)** The empirical distributions of mean-reverting time  $\tau$  in name space, with maximum empirical probability at  $\sim 6$  days (vertical dashed lines). **(b1-b6)** The empirical distributions of  $\tau$  in rank space, with maximum empirical probability at  $\sim 2.5$  days (vertical dashed lines). The residual returns in rank space show faster mean-reverting behavior, favorable for statistical arbitrage.

## 197 4.2 Portfolio performance

We present the PnL  $V_t$  in Fig. 5 with portfolio weights  $w_t^R$  are calculated by four scenarios: (i) the parametric benchmark model in name space in panel (a), (ii) the parametric benchmark model in rank space in panels (b,c), (iii) DNNs in name space in panel (d), and (iv) DNNs in rank space in panels (e, f). The corresponding Sharpe ratios from 2016 to 2022 are summarized in Fig. 5(g, h), with year-by-year statistics provided in Appendix G.1 (without transaction costs: Table 1; with transaction costs: Table 2).

The traditional statistical arbitrage strategy in name space using the parametric model exhibits diminishing profitability after the 2010s. In rank space, the parametric model yields mixed results: while initial performance without transaction costs appears attractive (Fig. 5(b)), accounting for transaction costs ( $\eta = 0.0002$ ) leads to a monotonic decline in PnL (Fig. 5(c)). **This stark contrast highlights a trade-off for statistical arbitrage in rank space: although the residual returns exhibit strong mean reversion and high profit potential, replicating these returns in rank space requires frequent intra-day rebalancing, which incurs substantial transaction costs.**

To address these challenges, we leverage DNNs to better exploit market patterns, particularly in rank space. The performance of DNNs in name and rank spaces diverges sharply. In name space, DNNs fail to improve returns or Sharpe ratios (Fig. 5(a, d); Appendix G.1, Table 1, Table 2). In contrast, in rank space, DNNs substantially enhance portfolio performance, achieving an average annual return of 35.68% and an average Sharpe ratio of 3.28 from 2007 to 2022 (Fig. 5(h); Table 2), even after accounting for transaction costs. This success is driven by the effective exploitation of mean-reversion behavior in rank space by DNNs that yields an average annual return of 206.49% and an average annual Sharpe ratio of 9.04 without transaction costs (Appendix G.1, Fig. 5(g), Table 1), sufficient to offset the substantial costs in intraday rebalancing to realize  $\tilde{r}_t$ .

Further characterization of the portfolios is provided in Appendix G. Appendix G.1 presents annualized performance statistics, Appendix G.2 examines market and dollar neutrality, Appendix G.3 discusses dependence on transaction costs, and Appendix G.4 analyzes the role of rank-swapping timescales on portfolio performance.

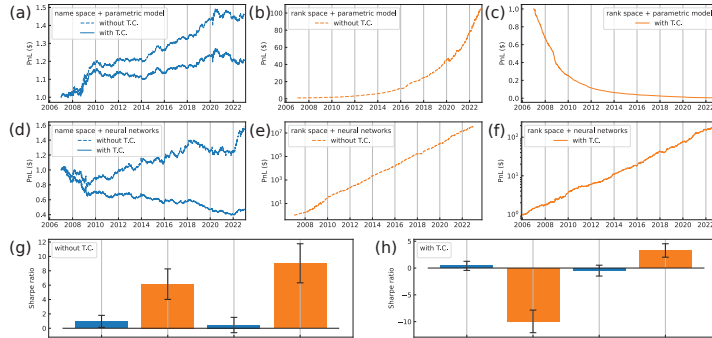


**Figure 5: Summary of portfolio performance.** The PnL dynamics  $V_t$  are computed using (3.15) in name space and (3.16) in rank space. **(a)** PnL using portfolio weights from the parametric model in name space; dashed and solid lines represent results without and with transaction costs, respectively. **(b, c)** PnL using portfolio weights from the parametric model in rank space; dashed/solid lines represent results without/with transaction costs in panel (b)/(c). **(d)** Same as (a), but using portfolio weights derived from DNNs in name space. **(e, f)** Same as (b, c), but using portfolio weights from DNNs in rank space. **(g, h)** Average Sharpe ratio without/with transaction costs shown in panel (g)/(h). Notably, portfolios derived from DNNs in rank space perform significantly better than those in name space.

### 224 4.3 The intelligence inside the neural networks

225 To understand the outperformance of DNNs compared to the benchmark parametric model in rank  
 226 space, we analyze the relationship between the input (the trajectories of the cumulative residual return  
 227  $x_t^L$ ) and the output (the portfolio weights in residual space  $w_t^\epsilon$ ).

228 We parameterize  $x_t^L$  by two key variables: the deviation from long-term average  $\frac{x_t - \mu}{\sigma}$ , and the  
 229 mean-reverting time  $\tau$ , following the trading signal suggested by the parametric model (E.4)). Each  
 230  $x_t^L$  thus corresponds to a point in the plane spanned by  $\frac{x_t - \mu}{\sigma}$  and  $\tau$ , color-coded by  $w_t^\epsilon$  (Fig. 6).

231 We evaluate four scenarios: (i) parametric model in name space (Fig. 6(a)), (ii) DNNs in name space  
 232 (Fig. 6(b)), (iii) parametric model in rank space (Fig. 6(d)), and (iv) DNNs in rank space (Fig. 6(e)).  
 233 We also report the average holding periods before liquidation for each method (Fig. 6(c, e)).

234 Compared to the parametric benchmark, the DNNs demonstrate more sophisticated trading behavior  
 235 in rank space. Despite operating directly on raw cumulative return trajectories, the DNNs successfully  
 236 uncover the significance of mean-reversion through mean-variance optimization (Fig. 6(e)). In  
 237 addition, the DNNs improve the execution strategy along three dimensions:

238 (i) Variable leverage on deviations. The DNNs assign higher leverage to positions with larger  
 239 normalized deviations  $\frac{x_t - \mu}{\sigma}$ , enhancing profit potential during significant market moves (Fig. 6(e)).

240 (ii) Flexible opportunity thresholds. Rather than relying on rigid mean-reversion time ( $\tau$ ) cutoffs as  
 241 in the parametric model (Fig. 6(a, d)), DNNs embrace a broader range of trading opportunities while  
 242 concentrating investments in trajectories with fast mean-reversion ( $\tau$  small) (Fig. 6(b, e)).

243 (iii) Shorter holding periods. DNNs reduce average holding periods to around 5 days, compared to  
 244 approximately 10 days under the parametric model (Fig. 6(c, e)). This minimizes carry-over risk,  
 245 which is particularly important when employing variable leverage across positions.

246 We also emphasize the critical role of market data preprocessing. While the DNNs achieve substantial  
 247 improvements in rank space, they fail to converge or deliver gains in name space (Fig. 7; Fig. 5(d)).  
 248 Despite both input spaces being derived from similar capitalization data, strategic reorganization into  
 249 rank space dramatically improves training efficiency (Fig. 7) and portfolio performance (Fig. 5). This  
 250 illustrates the importance of domain-informed data transformations in financial machine learning:  
 251 appropriate restructuring of the input space can substantially enhance the learning efficiency and  
 252 performance of deep models in complex, noisy environments like equity markets.

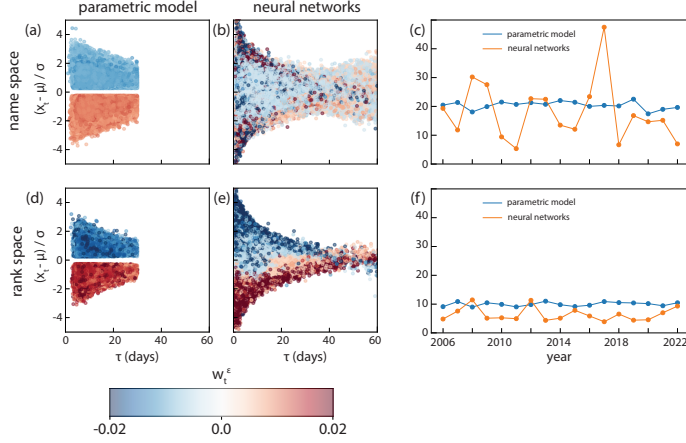


Figure 6: **Portfolio weights in residual space: parametric model versus neural networks.** (a, b, d, e) We illustrate the behavior of both the parametric model and neural networks by analyzing the relationship between the input, the trajectories of cumulative residual returns  $x_t^L$ , and the output, the portfolio weights in residual space,  $w_t^\epsilon$ . The input  $x_t^L$  are parameterized by two variables: (i) deviation from long-term average  $\frac{x_t - \mu}{\sigma}$ , and (ii) mean-reverting time  $\tau$ . Each  $x_t^L$  thus corresponds to a point in the plane spanned by  $\frac{x_t - \mu}{\sigma}$  and  $\tau$ , color-coded by  $w_t^\epsilon$ . This analysis is performed with  $w_t^\epsilon$  calculated by four scenarios: (a) the parametric model in name space; (b) neural networks in name space; (d) the parametric model in rank space; (e) neural networks in rank space. (c, f) Panel (c) and (f) show the average holding time for portfolios derived in name space and rank space, respectively. The DNN-derived portfolios exhibit more intelligence in terms of variable leverage, flexible opportunity thresholds, and shorter holding periods.

## 253 5 Limitations and discussion

254 Our current strategy is sensitive to transaction costs due to the frequent intraday rebalancing required  
 255 to realize return in rank space, as it ceases to profit with 5 bps transaction costs (Appendix G.3). The  
 256 induced transaction costs and slippage may limit the achievable volume and scalability in practice.  
 257 Furthermore, compared to a traditional parametric model in name space, portfolio weights derived  
 258 from neural networks exhibit significantly higher volatility (Figure 12 in Appendix G.2), raising  
 259 practical concerns for risk managements.

260 While our proposed intraday rebalancing mechanism (Appendix D) provides a baseline, it offers  
 261 substantial room for further optimization. Future work could formulate this challenge as a stochastic  
 262 control problem, leveraging physics-informed neural networks [24] to solve the resulting high-  
 263 dimensional partial differential equations, or alternatively as a reinforcement learning problem based  
 264 on real-market data.

265 The advantage of statistical arbitrage in rank space relies on frequent switching of ranks in capitalization,  
 266 resulting in a qualitatively different return space compared to that in name space. Therefore, we  
 267 expect that the advantage may generates to other volatile financial markets. Beyond financial markets,  
 268 the rank-based representation introduced here may generalize to other many-particle systems, such as  
 269 those encountered in many-particle physics[21], biology[8], and social sciences[12].

## 270 6 Conclusion

271 We have introduced a novel statistical arbitrage method that leverages the robust market structure  
 272 in rank space. Although rank space and name space contain the same underlying information,  
 273 the significant performance improvements achieved by DNNs in rank space highlight the critical  
 274 importance of domain-informed data representations in financial machine learning. In particular, our  
 275 results demonstrate how appropriate transformations of the input space can dramatically enhance  
 276 the learning efficiency and performance of deep models in complex, noisy environments such as  
 277 many-particle systems like equity markets.

278 **A Implementation details**

279 **A.1 Data and experimental setup**

280 We collect dividend-adjusted daily return, price, shares outstanding, and capitalizations for the U.S.  
 281 securities from Center for Research in Security Prices (CRSP), covering January 1990 to December  
 282 2022. Intraday price data at 1-minute resolution from January 2005 to December 2022 are obtained  
 283 from *Polygon.io*. We construct intraday capitalization data by combining CRSP shares outstanding  
 284 with *Polygon.io* intraday prices. The one-month Treasury bill rate from the Kenneth French Data  
 285 Library is used as the risk-free rate  $r_f$ .

286 **A.2 Calibrating investment universe and market decomposition**

287 Our backtesting spans January 2006 to December 2022, covering both the subprime mortgage crisis  
 288 and the highly competitive post-2010 market period. On each trading day after market close, we re-  
 289 calibrate the investment universe by selecting stocks that (i) rank among the top 500 in capitalization  
 290 as of day  $t$ , ensuring sufficient liquidity, and (ii) have valid historical return data available for day  
 291  $t + 1$ . This selection procedure minimizes potential selection bias to the best of our ability.

292 We then perform principal component analysis (PCA) on the selected returns using a 252-day  
 293 lookback window to extract leading eigenvectors as market factors  $F_t$ . Specifically, we retain the top  
 294 five eigenvectors (associated with the five largest eigenvalues) in name space, and the top eigenvector  
 295 in rank space. Factor loadings  $\beta_t$  are estimated using a 60-day lookback window, from which the  
 296 transformations  $\Phi_t$  and residual returns  $\epsilon_t$  are computed. Cumulative residual returns  $x_t^L$  are similarly  
 297 evaluated over the same 60-day window and are used as inputs to either the parametric benchmark  
 298 model (Appendix E) or the deep neural networks to generate portfolio weights and calculate the  
 299 resulting PnL.

300 **A.3 Deep neural networks**

301 We delve into the specific architecture of our neural networks, illustrated in Fig. 2. Our CNN-  
 302 transformer architecture harnesses the strengths of CNN in extracting local patterns and transformers  
 303 in capturing long-term dependencies. The inputs of our neural networks are the trajectories of  
 304 cumulative residual returns,  $x_t^L \in \mathbb{R}^{N \times L}$ , processed through two layer of multi-channel convolutional  
 305 networks, followed by a standard transformer encoder layer that models global relationships via  
 306 multi-head attention. Specifically, in the convolutionary layer,

$$\begin{aligned} x_t^{(1)} &= \frac{x_t^L - \mathbb{E}(x_t^L)}{\sqrt{\text{Var}(x_t^L) + \epsilon}} \times \gamma^{(1)} + \beta^{(1)}, & y_t^{(1)} &= W^{(1)} * x_t^{(1)} + b^{(1)}, & z_t^{(1)} &= \text{ReLU}(y_t^{(1)}) + x_t^{(1)}; \\ x_t^{(2)} &= \frac{z_t^{(1)} - \mathbb{E}(z_t^{(1)})}{\sqrt{\text{Var}(z_t^{(1)}) + \epsilon}} \times \gamma^{(2)} + \beta^{(2)}, & y_t^{(2)} &= W^{(2)} * x_t^{(2)} + b^{(2)}, & z_t^{(2)} &= \text{ReLU}(y_t^{(2)}) + x_t^{(2)}. \end{aligned} \quad (\text{A.1})$$

307 The superscript (1) or (2) specifies the layer number.  $x_t^{(1)} \in \mathbb{R}^{N \times L}$  is the input of the first convolu-  
 308 tional layer.  $W^{(1)} \in \mathbb{R}^{D_{\text{channel}} \times 1 \times D_{\text{kernel}}}$  and  $W^{(2)} \in \mathbb{R}^{D_{\text{channel}} \times D_{\text{channel}} \times D_{\text{kernel}}}$  are the convolutionary ker-  
 309 nels for the convolution operator denoted by  $*$ ,  $b^{(1,2)} \in \mathbb{R}^{D_{\text{channel}}}$  is the bias, and  $y_t^{(1,2)} \in \mathbb{R}^{N \times D_{\text{channel}} \times L}$   
 310 is the output of convolutionary operator.  $D_{\text{channel}}$  is the number of channels and  $D_{\text{kernel}}$  is the size of  
 311 the convolution kernel. We adopt a rectified linear unit (denoted as  $\text{ReLU}(\cdot)$ ) as our activation function.  
 312 We also apply (i) instance normalization [26] with learnable parameter  $\gamma^{(1,2)}$  and  $\beta^{(1,2)}$  at the input  
 313 of each convolution layer to accelerate the training process, and (ii) residual connection[15] to avoid  
 314 vanishing gradients by directly connecting the input  $x_t^{(1,2)}$  to the output  $z_t^{(1,2)} \in \mathbb{R}^{N \times D_{\text{channel}} \times T}$ . We  
 315 choose the hyper-parameters for our neural networks as number of channels  $D_{\text{channel}} = 8$  and size of  
 316 the convolution kernel  $D_{\text{kernel}} = 2$ .

317 The outputs of convolutionary layers,  $z_t^{(2)} \in \mathbb{R}^{N \times D_{\text{channel}} \times T}$  are subsequently fed into a standard  
 318 transformer encoder layer[27]. The transformer encoder layer utilizes the multi-head attention

319 modeled by the inner product between the famous key-query-value matrices. To elaborate,

$$\begin{aligned}
x_t^{\text{transformer}} &= (z_t^{(2)})^T \\
\begin{cases} Q_i \\ K_i \\ V_i \end{cases} &= \text{DropOut}(W_i^Q x_t^{\text{transformer}} + b_i^Q) \\
&= \text{DropOut}(W_i^K x_t^{\text{transformer}} + b_i^K), \quad i = 1, 2, \dots, H \\
&= \text{DropOut}(W_i^V x_t^{\text{transformer}} + b_i^V) \\
\text{head}_i &= \text{softmax}\left(\frac{Q_i K_i^T}{\sqrt{d_{\text{channel}}/H}}\right), \quad i = 1, 2, \dots, H \\
y_t &= \text{Concat}(\text{head}_1 V_1, \dots, \text{head}_H V_H) \\
z_t &= \text{LayerNorm}(x_t^{\text{transformer}} + y_t) \\
o_t &= \text{LayerNorm}(W^O z_t + b^O + y_t),
\end{aligned} \tag{A.2}$$

320 where  $x_t^{\text{transformer}} \in \mathbb{R}^{N \times T \times D_{\text{channel}}}$  is the input of the transformer encoder layer. In addition,  
321  $W_i^Q \in \mathbb{R}^{(D_{\text{channel}}/H) \times D_{\text{channel}}}$ ,  $W_i^K \in \mathbb{R}^{(D_{\text{channel}}/H) \times D_{\text{channel}}}$ , and  $W_i^V \in \mathbb{R}^{(D_{\text{channel}}/H) \times D_{\text{channel}}}$  are the  
322 linear weights.  $b_i^Q \in \mathbb{R}^{D_{\text{channel}}/H}$ ,  $b_i^K \in \mathbb{R}^{D_{\text{channel}}/H}$ , and  $b_i^V \in \mathbb{R}^{D_{\text{channel}}/H}$  are the bias. Softmax( $\cdot$ )  
323 stands for softmax function and Concat( $\cdot$ ) for matrix concatenation, and  $y_t \in \mathbb{R}^{N \times T \times D_{\text{channel}}}$  is the  
324 output of multi-attention layer.  $W^O \in \mathbb{R}^{D_{\text{channel}} \times D_{\text{channel}}}$  and  $b^O \in \mathbb{R}^{D_{\text{channel}}}$  are the linear weights and  
325 bias in the output linear layer.  $o_t \in \mathbb{R}^{N \times T \times D_{\text{channel}}}$  is the output of the transformer. In addition to the  
326 residual connection similar to the convolutional layer, we also introduce the drop-out technique, de-  
327 noted as DropOut( $\cdot$ ), to regularize overfitting with drop-out probability  $p$ , and layer normalization[5],  
328 denoted as LayerNorm( $\cdot$ ), to improve training stability. We choose the hyper-parameters for our  
329 neural networks as the number of heads  $H = 4$  and the drop-out probability  $p = 0.25$ .

330 Finally, we choose the last slice along the time axis in the output of the transformer,  $o_t \in$   
331  $\mathbb{R}^{N \times T \times D_{\text{channel}}}$ , as the hidden state summarizing the information up to time  $t$ . The portfolio weights  
332 in residual space  $w_t^{\epsilon|\text{NN}, \text{name/rank}}$  are calculated by a linear relationship,

$$w_t^{\epsilon|\text{NN}, \text{name/rank}} = W^F(o_t[:, -1, :]) + b^F, \tag{A.3}$$

333 where  $o_t[:, -1, :] \in \mathbb{R}^{N \times D_{\text{channel}}}$  means the last slice along the second-dimension (time-axis) of  $o_t$ , and  
334  $W^F \in \mathbb{R}^{1 \times D_{\text{channel}}}$ ,  $b^F \in \mathbb{R}$  are the parameters.

335 For the mean-variance optimization target in (3.10), the empirical expectation and variance are  
336 obtained over a consecutive time window of length  $T$ ,

$$\begin{aligned}
\mathbb{E}[(w_t^{R|\text{NN}})^T (r_{t+1} - r_f)] &\approx \frac{1}{T} \sum_{\alpha=1}^T (w_{t+\alpha}^{R|\text{NN}})^T (r_{t+\alpha+1} - r_f) \\
\text{Var}[(w_t^{R|\text{NN}})^T (r_{t+1} - r_f)] &\approx \frac{1}{T} \sum_{\alpha=1}^T [(w_{t+\alpha}^{R|\text{NN}})^T (r_{t+\alpha+1} - r_f) - \mathbb{E}((w_t^{R|\text{NN}})^T (r_{t+1} - r_f))]^2
\end{aligned} \tag{A.4}$$

337 We choose the risk-aversion factor  $\gamma = 2$  and length of time window  $T = 24$  days.

338 The neural networks are trained in two steps. The first step aims at optimizing the hyper-parameters  
339 of neural network. Specifically, to evaluate the portfolio weights from the trading day  $t$  to day  $t + 252$ ,  
340 we utilize the data from  $t - 1000$  to  $t - 60$  as the training data set and from  $t - 59$  to  $t - 1$  as the  
341 validation data set, from which we determine hyper-parameters from the converged mean-variance  
342 target in the training curve (Fig. 7). The hyperparameters of our optimized neural network architecture  
343 are elaborated in Appendix A.3.

344 The second step aims at increasing the updating frequency of parameters in the neural networks from  
345 annually to quarterly while keeping hyper-parameters fixed. More explicitly, to evaluate the portfolio  
346 weights from the trading day  $t$  to day  $t + 63$ , we use the data from trading day  $t - 500$  to day  $t - 1$  as the  
347 training data set. Empirically, increasing the updating frequency is significantly beneficial  
348 to the performance of neural network, due to the non-stationarity in financial data. The training  
349 tasks utilize PyTorch 2.2.0, and are parallelized on a workstation with a CPU from AMD Ryzen  
350 Threadripper Pro 5955 WX and two GPUs from Nvidia GeForce RTX 4090. **Each neural network**  
351 **training iteration takes approximately two hours to converge, resulting in roughly 130 computational**

352 hours for backtesting portfolio performance from 2007 to 2022, assuming quarterly neural network  
 353 retraining. In our rank-space statistical arbitrage strategy, the daily portfolio weights in rank space  
 354 are precomputed by forward propagation of the neural network before market opening, and remain  
 355 fixed during the trading day. To handle rank changes, the intraday rebalancing of portfolio weights  
 356 from rank space to name space occurs every 225 minutes.

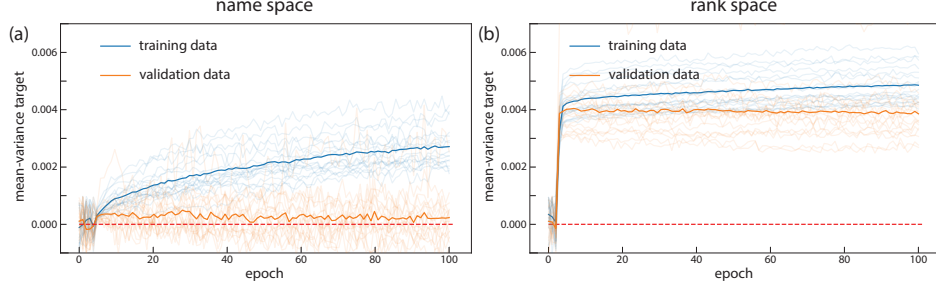


Figure 7: Training curves of neural networks. **(a, b)** We show the mean-variance target as a function of training epochs for neural networks as specified by (3.10) in name space (a) and in rank space (b). The training curves originate from the phase I training process focusing on hyperparameter tuning. To evaluate the out-of-sample portfolio weights from trading day  $t$  to  $t + 252$ , we use the training data from day  $t - 1000$  to day  $t - 60$  and validation data from day  $t - 59$  to  $t - 1$  as the validation data. The neural networks are re-trained annually with random initialization, yielding approximately 17 training curves from 2006 to 2022. The transparent lines show individual training curves with their average represented by the opaque lines. The neural networks in rank space are more efficiently trained than those in name space.

358 We provide implementation details in the form of pseudocode. Algorithm 1 performs market  
 359 decomposition in both name and rank space, as discussed in section 3.1. Algorithm 2 calculates  
 360 the portfolio weights using the parametric model (section E), while algorithm 3 does so via neural  
 361 networks (section 3.2 and A.3). Algorithm 4 handles the conversion of portfolio weights between  
 362 name space and rank space (section D). Algorithm 5 computes the summary statistics of portfolio  
 363 performance reported in 1 and 2. Finally, algorithm 6 and 7 integrate the proposed algorithmic  
 364 components above to implement the complete statistical arbitrage strategy in name and rank space,  
 365 respectively.

---

**Algorithm 1** Market decomposition (PCA) [Fig. 1, panel(c1, c2)]

---

**Input:**  $r_t, r_{f,t}, K$   
**Output:**  $\epsilon_t, \Phi_t$

**Function** market\_decomposition( $r_t, r_{f,t}, K$ ):

Principal component analysis:  $r_t - r_{f,t} = U\Sigma V^T$   
 $F_t \leftarrow (v_1, v_2, \dots, v_K)$ , where  $v_k$  is the  $k$ -th column of  $V^T$   
 Calculate  $\omega_t$  by solving  $F_t = \omega_t(r_t - r_f)$   
 Calculate  $\beta_t$  as the coefficient of the linear regression  $r_t - r_f \sim F_t$   
 $\Phi_t \leftarrow I - \beta_t \omega_t$   
 $\epsilon_t \leftarrow \Phi_t(r_t - r_{f,t})$   
**return**  $\epsilon_t, \Phi_t$

// Input:  
 //  $r_t$ : return in name space or transformed return in rank space.  
 //  $r_{f,t}$ : risk-free rate at the end of trading day  $t$ .  
 //  $K$ : number of market factors, predetermined by analyzing eigenvalue  
 // spectrum of the correlation matrix.  
// Output:  
 //  $\epsilon_t$ : residual returns in name space or rank space.  
 //  $\Phi_t$ : transformation between residual space and equity space  
 // ((3.1) for name space and (3.6) for rank space).  
// Note:  
 // The algorithm realizes the formulation in section 2.1.  
 // Factors  $F_t$  and  $\omega_t$  are calculated on a 252-day look-back window.  
 // Loadings  $\beta_t$  are calculated on a 60-day look-back window.  
 //  $F_t$ ,  $\omega_t$ , and  $\beta_t$  are updated daily.  
 //  $K = 5$  for name space and  $K = 1$  for rank space based on empirical  
 // eigenvalue spectrum of the correlation matrix (Fig. 3(c,d))).

---

---

**Algorithm 2** Portfolio weights by parametric model [Fig. 1, panel(d1, e1)]

---

**Input:**  $\epsilon_t, \Phi_t$   
**Output:**  $w_t^{R|OU}$

**Function** portfolio\_weights\_by\_parametric\_model( $\epsilon_t, \Phi_t$ )  
 Calculate  $x_t^L$  by (3.9)  
 Estimate  $\tau, \mu, \sigma, x_t, R^2$  by fitting  $x_t^L$  to an OU process ((E.1))  
 Calculate  $w_t^{\epsilon|OU}$  by (E.4)  
 $w_t^{R|OU} \leftarrow \Phi_t^T w_t^{\epsilon|OU}$  ((E.7))  
**return**  $w_t^{R|OU} / \|w_t^{R|OU}\|_1$

// Input:  
//  $\epsilon_t$ : residual returns calculated from Algorithm 1  
//  $\Phi_t$ : transformation matrix between equity space and residual space  
from  
 // Algorithm 1  
// Output:  
//  $w_t^{R|OU}$ :  $l_1$ -normalized portfolio weights by parametric model.  
 // For name space, it stands for the portfolio weights on stocks.  
 // For rank space, it corresponds to the portfolio weights on  
 // artificial financial instruments that realize rank returns  
 // defined in (3.5).  
// Note:  
 // The algorithm realizes the formulation in section 2.2.1.  
 //  $\tau, \mu, \sigma$  are fitting parameters of OU process.  
 // Risk control by ignoring  $\tau > 30$  days ((E.4)).

---



---

**Algorithm 3** Portfolio weights by neural networks [Fig. 1, panel(d2, e2)]

---

**Input:**  $\epsilon_t, \Phi_t$   
**Output:**  $w_t^{R|NN}$

**Function** portfolio\_weights\_by\_neural\_networks( $\epsilon_t, \Phi_t$ )  
 Calculate  $x_t^L$  by (3.9)  
 Train neural network in-sample for mean-variance optimization ((3.10))  
 Calculate  $w_t^{\epsilon|NN}$  out-of-sample from trained neural network  
**return**  $w_t^{R|NN} / \|w_t^{R|NN}\|_1$

// Input:  
//  $\epsilon_t$ : residual returns calculated from Algorithm 1.  
//  $\Phi_t$ : transformation matrix between equity space and residual space  
from  
 // Algorithm 1.  
// Output:  
//  $w_t^{R|NN}$ :  $l_1$ -normalized portfolio weights by parametric model.  
 // For name space, it stands for the portfolio weights on stocks.  
 // For rank space, it corresponds to the portfolio weights on  
 // artificial financial instruments that realize rank returns.  
 // defined in (3.5).  
// Note:  
 // The algorithm realizes the formulation in section 2.2.2.  
 // No pre-screening on trading opportunities  $x_t^L$  applied.  
 // Neural networks internally prioritize various trading opportunities  
 // and manage risk (Fig. 6).  
 // The mean-variance target is evaluated on a 24-day window.

---

---

**Algorithm 4** intraday rebalancing [Fig. 1, panel (f3)]

---

**Input:**  $w_t^R, r_{f,t}, \mathcal{T}$   
 $c_{t+\tau}, \quad t = 1, 2, \dots, T$  (days),  $\tau = 1, 2, \dots, N$  (minutes)

**Output:**  $V_t, \quad t = 1, 2, \dots, T + 1$

**Function** intraday\_rebalancing( $w_t^R, r_{f,t}, \mathcal{T}, c_{t+\tau}$ )

$t \leftarrow 0, V_t \leftarrow 1, w^{\text{prev}} \leftarrow 0$

**While**  $t \leq T$  ▷  $T$  is daily time tick

$w_{(k),t}^{\text{rank}} \leftarrow w_{(k),t}^R, \quad k = 1, 2, \dots, N$

$w_{\mathcal{I}_{(k),t},t}^{\text{name}} \leftarrow w_{(k),t}^R, \quad k = 1, 2, \dots, N$  ▷  $\mathcal{I}_{(k),t}$  maps from rank to name

$V_t \leftarrow V_t - \sum_i w_{i,t}^{\text{name}} - 0.0002 \times \|w_t^{\text{name}} - w^{\text{prev}}\|_1$

$\tau \leftarrow 0$

**While**  $t + \tau < (t + 1)$  ▷  $\tau$  is intraday time tick

$w_{(k),t+\tau}^{\text{rank}} \leftarrow w_{(k),t+\tau-1}^{\text{rank}} \times \frac{c_{(k),t+\tau}}{c_{(k),t+\tau-1}}, k = 1, 2, \dots, N$  ((3.12))

$w_{i,t+\tau}^{\text{name}} \leftarrow w_{i,t+\tau-1}^{\text{name}} \times \frac{c_{i,t+\tau}}{c_{i,t+\tau-1}}, i = 1, 2, \dots, N$  ((3.13))

▷  $t + \tau - 1$  and  $t + \tau$  are adjacent intraday timestamps

**if**  $\tau \% \mathcal{T} == 0$  **or** end of the trading day ▷ rebalancing point

Calculate cost( $t + \tau, w_{(k),t}^{\text{rank}}$ ) by (3.14)

$V_t \leftarrow V_t - \text{cost}(t + \tau, w_{(k),t}^{\text{rank}})$

$w_{\mathcal{I}_{(k),t+\tau},t+\tau}^{\text{name}} \leftarrow w_{(k),t+\tau}^{\text{rank}}, \quad k = 1, 2, \dots, N$

$\tau \leftarrow \tau + 1$

$V_{t+1} \leftarrow (1 + r_{f,t+1})V_t + \sum_i w_{i,t+\tau}^{\text{name}}$

$w^{\text{prev}} \leftarrow w_{t+\tau}^{\text{name}}$

$t \leftarrow t + 1$

**return**  $V_t, \quad t = 1, 2, \dots, T + 1$

// Input:

//  $w_t^R$ : the  $l_1$ -normalized portfolio weights from either parametric  
// model (Algorithm 2) or neural networks (Algorithm 3).

//  $r_{f,t}$ : risk-free rate during the trading day  $t$ .

//  $\mathcal{T}$ : rebalance interval.

//  $c_{t+\tau}$ : the capitalization processes in name space and rank space at  
// 1-minute resolution throughout the trading day  $t$ .  
//  $t$  is the time tick at daily level.  
//  $\tau$  is the time tick at minute level.

// Output:

//  $V_t$ : the value process of the portfolio (PnL) with weights  $w_t^R$ .

// Note:  
// The algorithm realizes the formulation in section 2.3.1.  
// In essence, it converts portfolio weights from rank to name  
// at  $\mathcal{T}$  minutes interval.

---

---

**Algorithm 5** portfolio metric [Fig. 1, panel (g)]

---

**Input:**  $V_t$ ,  $t = 1, 2, \dots, N$   
**Output:**  $r_{\text{annual}}$ ,  $\sigma_{\text{annual}}$ ,  $\text{SR}_{\text{annual}}$

```

Function portfolio_metric( $V_t, r_f$ )
  For year in years_in_backtesting:
    Locate all  $t_1 \leq t_2 \leq \dots \leq t_N$  in year
     $r_{t_i} = V_{t_i}/V_{t_{i-1}} - 1$ ,  $i = 1, 2, \dots, N$ 
     $r_{\text{annual}} \leftarrow (\prod_{i=1}^N (1 + r_{t_i}))^{252/N} - 1$ 
     $\sigma_{\text{annual}} \leftarrow \sqrt{252} \times \text{std}(\{r_{t_i}\}_{i=1}^N)$   $\triangleright$  std is the standard deviation
     $\text{SR}_{\text{annual}} \leftarrow (r_{\text{annual}} - r_{f,\text{annual}})/\sigma_{\text{annual}}$   $\triangleright r_{f,\text{annual}}$  is annualized risk-free rate
  return  $r_{\text{annual}}, \sigma_{\text{annual}}, \text{SR}_{\text{annual}}$  for all backtesting years

// Input:
//  $V_t$ : the value process (PnL) of the portfolio with weights  $w_t^R$ .
//  $r_{f,t}$ : the risk-free rate at the end of trading day  $t$ .
// Output:
// The algorithm realizes the formulation in section 2.4.
//  $r_{\text{annual}}$ : the annualized return for all backtesting years.
//  $\sigma_{\text{annual}}$ : the annualized volatility for all backtesting years.
//  $\text{SR}_{\text{annual}}$ : the Sharpe ratio for all backtesting years.

```

---



---

**Algorithm 6** (Integrated) Statistical arbitrage in name space

---

**Input:**  $r_t, r_f, K$   
**Called algorithm:** Algorithm 1, Algorithm 2, Algorithm 3, Algorithm 5  
**Output:**  $w_t^R, V_t, \text{SR}_{\text{annual}}$

```

Function statistical_arbitrage_in_name_space( $r_t, r_{f,t}, K$ )
   $\epsilon_t, \Phi_t \leftarrow \text{market_decomposition}(r_t, r_{f,t}, K)$  from Algorithm 1
  if parametric model
     $w_t^{R|\text{OU}} \leftarrow \text{portfolio_weights_by_parametric_model}(\epsilon_t, \Phi_t)$  from Algorithm 2;
  if neural networks
     $w_t^{R|\text{NN}} \leftarrow \text{portfolio_weights_by_neural_network}(\epsilon_t, \Phi_t)$  from Algorithm 3
  Calculate PnL  $V_t$  by (3.15)
   $r_{\text{annual}}, \sigma_{\text{annual}}, \text{SR}_{\text{annual}} \leftarrow \text{portfolio_metric}(V_t, r_{f,t})$  from Algorithm 5
  return  $w_t^R, V_t, \text{SR}_{\text{annual}}$ 

// Input:
//  $r_t$ : dividend-adjusted daily return in name space.
//  $r_{f,t}$ : risk-free rate at the end of trading day  $t$ .
//  $K$ : number of market factors, predetermined by analyzing
eigenvalue
  // spectrum of the correlation matrix.
// Output:
//  $w_t^R$ : the  $l_1$ -normalized portfolio weights on stock.
//  $V_t$ : the value process (PnL) of the portfolio with weights  $w_t^R$ .
//  $r_{\text{annual}}, \sigma_{\text{annual}}, \text{SR}_{\text{annual}}$ : annualized return, volatility, and Sharpe
  // ratio.

```

---

---

**Algorithm 7** (Integrated) Statistical arbitrage in rank space

---

**Input:**  $c_t, c_{t+\tau}, r_f, K$   
**Called algorithm:** Algorithm 1, Algorithm 2, Algorithm 3, Algorithm 4, Algorithm 5  
**Output:**  $w_t^R, V_t, r_{\text{annual}}, \sigma_{\text{annual}}, \text{SR}_{\text{annual}}$

```

Function statistical_arbitrage_in_name_space( $c_t, r_{f,t}, K$ )
    Calculate  $\tilde{r}_t$  by (3.5)
     $\tilde{\epsilon}_t, \tilde{\Phi}_t \leftarrow \text{market\_decomposition}(\tilde{r}_t, r_{f,t}, K)$  from Algorithm 1
    if parametric model
         $w_t^{R|\text{OU}} \leftarrow \text{portfolio\_weights\_by\_parametric\_model}(\epsilon_t, \Phi_t)$  from Algorithm 2;
    if neural networks
         $w_t^{R|\text{NN}} \leftarrow \text{portfolio\_weights\_by\_neural\_network}(\epsilon_t, \Phi_t)$  from Algorithm 3
     $V_t \leftarrow \text{intraday\_rebalancing}(w_t^{R|\text{NN}}, r_{f,t}, \mathcal{T}, c_{t+\tau})$  from Algorithm 4
     $r_{\text{annual}}, \sigma_{\text{annual}}, \text{SR}_{\text{annual}} \leftarrow \text{portfolio\_metric}(V_t, r_{f,t})$  from Algorithm 5
    return  $w_t^R, V_t, r_{\text{annual}}, \sigma_{\text{annual}}, \text{SR}_{\text{annual}}$ 

    // Input:
    //  $c_t$ : capitalizations at the end of trading day  $t$ .
    //  $c_{t+\tau}$ : capitalization process at 1-minute resolution throughout the
    // trading day  $t$ .  $t$  is the time tick at daily level.
    //  $\tau$  is the time tick at intraday level.
    //  $r_{f,t}$ : risk-free rate at the end of trading day  $t$ .
    //  $K$ : number of market factors, predetermined by analyzing
    eigenvalue
    // spectrum of the correlation matrix.
    // Output:
    //  $w_t^R$ : the  $l_1$ -normalized portfolio weights on artificial financial
    // instruments that realize  $\tilde{r}_t$ .
    //  $V_t$ : the value process (PnL) of the portfolio with weights  $w_t^R$ .
    //  $r_{\text{annual}}, \sigma_{\text{annual}}, \text{SR}_{\text{annual}}$ : annualized return, volatility, and Sharpe
    // ratio.

```

---

366 **B Hybrid-Atlas model**

367 In this section, we introduce a hybrid-Atlas model that motivates the definition of return in (3.5) and  
 368 hints at the qualitative difference between name space and rank space[7, 6, 18].

369 We study an equity market that consists of  $n$  stocks with capitalizations  $C(t) = (C_1(t), \dots, C_n(t))$ ,  
 370 where  $C_i(t)$  represents the capitalization at time  $t$  of the asset with name  $i$ . We assume that the  
 371 log-capitalizations  $Y_i(t) := \log C_i(t)$ ,  $i = 1, \dots, n$ , satisfy the system of stochastic differential  
 372 equations:

$$dY_i(t) = (g_{R_{i,t}} + \gamma_i + \gamma) dt + \sum_{j=1}^n \rho_{i,j} dW_j(t) \\ + \sigma_{R_{i,t}} Y_i(t) dW_i(t), \quad Y_i(0) = y_i, \quad 0 \leq t < \infty \quad (\text{B.1})$$

373 with given initial condition  $y = (y_1, \dots, y_n)'$ . We assume that  $\gamma = 0$  and the system satisfies the  
 374 stability condition

$$\sum_{k=1}^n g_k + \sum_{i=1}^n \gamma_i = 0. \quad (\text{B.2})$$

375 Define the log-capitalization process in rank space,  $Z_k(t) = Y_{\mathcal{I}_{k,t}}(t)$ . Therefore, the rank return  
 376 defined in (3.5) can be viewed as the discrete counterpart of  $dZ_k(t)$ .

377 Theorem B.3 highlights the qualitative difference between residual rank space and name space beyond  
 378 linear transformation.

379 **Lemma B.1.** *For continuous semimartingales  $Y_1, Y_2, \dots, Y_n$ , the rank process  $Z_1, Z_2, \dots, Z_n$  are  
 380 continuous semimartingales, and we have*

$$\sum_{k=1}^n L_t(Z_k) = \sum_{i=1}^n L_t(Y_i), \quad \forall t > 0, \quad (\text{B.3})$$

381 where  $L_t(Y) = \frac{1}{2\epsilon} \int_0^t \mathbf{1}_{\{-\epsilon < Y_s < \epsilon\}} dY_s$  is the local time accumulated at origin.

382 *Proof.* The proof follows [6] theorem 2.2. □

383 **Lemma B.2.** *For continuous semimartingales  $Y_1, Y_2, \dots, Y_n$  and their rank process  $Z_1, Z_2, \dots, Z_n$ ,  
 384 we have*

$$dZ_k(t) = \sum_{i=1}^n (N_k(t))^{-1} \mathbf{1}_{\{Z_k(t)=X_i(t)\}} dX_i(t) \\ + \sum_{j=k+1}^n (N_k(t))^{-1} dL_t(Z_k - Z_j) - \sum_{j=1}^{k-1} (N_k(t))^{-1} dL_t(Z_j - Z_k). \quad (\text{B.4})$$

385 , where  $S_t(k) := \{i : Y_i(t) = Z_k(t)\}$  and  $N_k(t)$  is the cardinality of  $S_t(k)$ .

386 *Proof.* Our proof follows [6] theorem 2.3 closely.

387 Define

$$U = \{u(\cdot) : \mathbb{R}^+ \times \{1, \dots, n\} \rightarrow \{1, \dots, n\}, Z_k(t) = Y_{u_t(k)}(t), \forall t > 0, k = 1, \dots, n\}. \quad (\text{B.5})$$

388 For any  $j \in J$ , we define  $u^j$  of  $U$  as

$$u_t^j(k) := \text{the } j_{N_t(k)}\text{-th smallest element of } S_t(k). \quad (\text{B.6})$$

389 In other words, suppose that at time  $t$  precisely  $m$  of the processes  $X_1, \dots, X_n$  have rank  $k$ , denoted  
 390 as  $X_{i_1}, \dots, X_{i_m}$ . Then,  $u_t^j(k)$  is the  $j_m$ -th smallest among the indices  $i_1, \dots, i_m$ .

391 For  $u \in U$ , we have

$$\begin{aligned}
Z_k(t) - Z_k(0) &= \sum_{i=1}^n \int_0^t \mathbf{1}_{\{u_s(k)=i\}} dY_i(s) + \sum_{i=1}^n \int_0^t \mathbf{1}_{\{u_s(k)=i\}} d(Z_k(s) - Y_i(s)) \\
&= \frac{1}{n!} \sum_{i=1}^n \int_0^t \sum_{j \in J} \mathbf{1}_{\{u_s^j(k)=i\}} dY_i(s) + \frac{1}{n!} \sum_{i=1}^n \int_0^t \sum_{j \in J} \mathbf{1}_{\{u_s^j(k)=i\}} d(X_{(k)}(s) - X_i(s)) \\
&= \sum_{i=1}^n \int_0^t (N_s(k))^{-1} \mathbf{1}_{\{Z_k(s)=Y_i(s)\}} dY_i(s) + \sum_{i=1}^n \int_0^t (N_s(k))^{-1} \mathbf{1}_{\{Z_k(s)=Y_i(s)\}} d(Z_k(s) - Y_i(s)) \\
&= \sum_{i=1}^n \int_0^t (N_s(k))^{-1} \mathbf{1}_{\{Z_k(s)=Y_i(s)\}} dY_i(s) + \sum_{i=1}^n \int_0^t (N_s(k))^{-1} dL_s((Z_k - Y_i)^+) \\
&\quad - \sum_{i=1}^n \int_0^t (N_s(k))^{-1} dL_s((Z_k - Y_i)^-).
\end{aligned} \tag{B.7}$$

392 , where  $(\cdot)^+ = \max(\cdot, 0)$  and  $(\cdot)^- = \min(\cdot, 0)$ . In the second equality, we replace  $u$  by  $u^j$  for  $j \in J$ ,  
393 then summing over all  $j$ . In the third equality, we use  $\sum_{j \in J} \mathbf{1}_{\{u_s^j(k)=i\}} = \frac{n!}{N_s(k)} \mathbf{1}_{\{X_{(k)}(s)=X_i(s)\}}$ .  
394 In the fourth equality, we use lemma B.1 and

$$\begin{aligned}
&\sum_{i=1}^n \int_0^t (N_s(k))^{-1} \mathbf{1}_{\{Z_k(s)=Y_i(s)\}} d(Z_k(s) - Y_i(s)) \\
&= \sum_{i=1}^n \int_0^t (N_s(k))^{-1} \mathbf{1}_{\{Z_k(s)=Y_i(s)\}} d((Z_k(s) - Y_i(s))^+) \\
&\quad - \sum_{i=1}^n \int_0^t (N_s(k))^{-1} \mathbf{1}_{\{Z_k(s)=Y_i(s)\}} d((Z_k(s) - Y_i(s))^-) \\
&= \sum_{i=1}^n \int_0^t (N_s(k))^{-1} dL_s((Z_k - Y_i)^+) - \sum_{i=1}^n \int_0^t (N_s(k))^{-1} dL_s((Z_k - Y_i)^-).
\end{aligned} \tag{B.8}$$

395  $\square$

396 **Theorem B.3.** *The log-capitalization process in rank space  $Z_k$  satisfies*

$$\begin{aligned}
dZ_k(t) &= (g_{\mathcal{R}_{i,t}} + \gamma_i + \gamma) dt + \sum_{j=1}^n \rho_{i,j} dW_j(t) + \sigma_{\mathcal{R}_{i,t}} Y_i(t) dW_i(t), dY_{\mathcal{I}_{k,t}}(t) \\
&\quad + \frac{1}{2}(d\Lambda^{k,k+1}(t) - d\Lambda^{k-1,k}(t))
\end{aligned} \tag{B.9}$$

397 , where  $\Lambda^{k,k+1}$  is the local time accumulated at the origin by the non-negative semimartingale  
398  $Z_k(t) - Z_{k+1}(t)$  defined as

$$\Lambda^{k,k+1}(t) = \lim_{\varepsilon \downarrow 0} \frac{1}{2\varepsilon} \int_0^t \mathbf{1}_{\{-\varepsilon < Z_k(s) - Z_{k+1}(s) < \varepsilon\}} d(Z_k(s) - Z_{k+1}(s)) \tag{B.10}$$

399 *Proof.* From the lemmas above, we have

$$\begin{aligned}
dZ_k(t) &= (g_{\mathcal{R}_{i,t}} + \gamma_i + \gamma) dt + \sum_{j=1}^n \rho_{i,j} dW_j(t) + \sigma_{\mathcal{R}_{i,t}} Y_i(t) dW_i(t), dY_{\mathcal{I}_{k,t}}(t) \\
&\quad + (N_k(t))^{-1} \left[ \sum_{\ell=k+1}^n d\Lambda^{k,\ell}(t) - \sum_{\ell=1}^{k-1} d\Lambda^{\ell,k}(t) \right] \\
&= (g_{\mathcal{R}_{i,t}} + \gamma_i + \gamma) dt + \sum_{j=1}^n \rho_{i,j} dW_j(t) + \sigma_{\mathcal{R}_{i,t}} Y_i(t) dW_i(t), dY_{\mathcal{I}_{k,t}}(t) \\
&\quad + \frac{1}{2}(d\Lambda^{k,k+1}(t) - d\Lambda^{k-1,k}(t))
\end{aligned} \tag{B.11}$$

400 , where the second equality follows from [18] lemma 1 that the local times  $\Lambda^{k,l}$  generated by triple or  
401 higher-order collisions are identically equal to zero. In other words,  $\Lambda^{k,l} = 0$  for  $|k - l| \geq 2, 1 \leq$   
402  $k, l \leq n$ .  $\square$

403 **C Market neutrality**

404 The statistical arbitrage portfolios need to satisfy the market neutrality constraint,  $w^T \beta = 0$ , so that  
 405 the return of the portfolio is independent of market factors

$$w^T(r_t - r_f) = w^T(\beta_t F_t + \epsilon_t) = w^T \epsilon_t. \quad (\text{C.1})$$

406 The following theorem proves that the market neutrality of the portfolio constructed in section 3.1  
 407 satisfies the constraints.

408 **Theorem C.1.** *If the portfolio weights satisfies Eq. 3.4 or Eq. 3.8, it is market neutral.*

409 *Proof.* We denote the return matrix  $R_t = (r_{t-T+1}, r_{t-T+2}, \dots, r_t) \in \mathbb{R}^{N \times T}$ . Assume singular value  
 410 decomposition of  $R_t - R_f$ ,

$$R_t - R_f = U \Sigma V^T \quad (\text{C.2})$$

411 , where  $R_f \in \mathbb{R}^{1 \times T}$  is the risk-free rate,  $U \in \mathbb{R}^{N \times N}$ ,  $\Sigma \in \mathbb{R}^{N \times T}$ , and  $V^T \in \mathbb{R}^{T \times T}$ . Then, the  
 412 factors and loadings in Eq. 3.1 and  $\omega_t$  in Eq. 3.2 becomes

$$F_t = \begin{pmatrix} v_1^T \\ v_2^T \\ \vdots \\ v_K^T \end{pmatrix}, \quad \beta_t = (u_1, u_2, \dots, u_K) \begin{pmatrix} \sigma_1 & & \\ & \ddots & \\ & & \sigma_K \end{pmatrix}, \quad \omega_t = \begin{pmatrix} \sigma_1^{-1} & & \\ & \ddots & \\ & & \sigma_K^{-1} \end{pmatrix} \begin{pmatrix} u_1^T \\ u_2^T \\ \vdots \\ u_K^T \end{pmatrix} \quad (\text{C.3})$$

413 , where  $u_i$  and  $v_i$  are the  $i$ -th column of matrix  $U$  and  $V$ . Then, due to the orthogonality between  $U$   
 414 and  $V$ ,

$$\Phi_t \beta_t = (I - \beta_t \omega_t) \beta_t = \beta_t - \beta_t (\omega_t \beta_t) = \beta_t - \beta_t = 0, \quad (\text{C.4})$$

415 . Therefore,

$$(w_t^R)^T \beta = (w_t^\epsilon)^T \Phi_t \beta = 0 \quad (\text{C.5})$$

416  $\square$

417 **D Intraday rebalancing**

418 The portfolio weights calculated in the rank space are assigned to artificial financial instruments  
 419 that yield rank returns in continuous-time limits defined in (3.5). To make the constructed portfolio  
 420 practically implementable, it is necessary to convert these portfolio weights into stock-based portfolios  
 421 in name space.

422 A naive approach is to assign the portfolio weights with correspondence between ranks and names at  
 423 the end of each trading day and hold the portfolio throughout the following trading day,

$$w_{i,t} = \sum_{k=1}^N w_{(k),t} \mathbf{1}_{\{\mathcal{R}_{i,t}=k\}}, \quad i = 1, 2, \dots, N. \quad (\text{D.1})$$

424 Unfortunately, this straightforward conversion will not retain the advantages of statistical arbitrage in  
 425 rank space, because the performance of the derived portfolio will essentially still depend on returns  
 426 in name space rather than the rank returns in continuous-time limit. As indicated by (3.5), the returns  
 427 in name and rank space start to diverge in the event of rank switching that frequently occurs for most  
 428 ranks at an intraday frequency. It indicates that an effective conversion strategy must appropriately  
 429 respond to the rank-switching events.

430 Consequently, we propose an intraday rebalancing mechanism in section 3.3. This mechanism  
 431 performs conversion from rank space to name space at a frequency that matches rank-switching  
 432 events, even though it results in higher transaction costs due to more frequent trading. In the following,  
 433 we carry out an in-depth analysis in a two-stock system to emphasize the crucial role of rank switching  
 434 and the rebalancing interval in determining the cost of conversion.

435 **D.1 Portfolio rebalancing through rank switching of two stocks**

436 To elucidate the pivotal role of rank switching in our intraday rebalancing strategy, we examine a  
 437 two-stock system depicted in Fig. 8, where the two capitalization processes  $c_{t,1}$  and  $c_{t,2}$  maintain  
 438 their ranks during the rebalancing interval  $((k-1)\mathcal{T}, k\mathcal{T}], k \in \mathbb{N}$  and swap their ranks during  
 439  $(k\mathcal{T}, (k+1)\mathcal{T}], k \in \mathbb{N}$  (panels (a1-a7)). The red lines in panels (b1-b7) and green lines in panels  
 440 (c1-c7) show the dollar portfolio weight on the stock that occupies  $k$ -th rank in capitalization,  
 441  $w_{(k),\tau}, k = 1, 2$ . The orange lines in panels (b1-b7) and blue lines in panels (c1-c7) show the dollar  
 442 portfolio weight on the stock that has  $i$ -th name index,  $w_{i,\tau}, i = 1, 2$ . We further calculate and present  
 443 in panels (d1-d7) the divergence between the total dollar portfolio weights in rank space and the total  
 444 dollar portfolio weights in name space, defined as  $w_{(1),t} + w_{(2),t} - w_{1,t} - w_{2,t}$ . Panels (e1-e7) shows  
 445 the cumulative cost from the bid-ask spread arising from the active trading at the rebalancing point.  
 446 We highlight several representative timestamps elaborated below.

447 (i)  $t = (k-1)\mathcal{T}^+$  in panels (a1-e1): We invest  $w_{(2),t}$  on stock 1 and  $w_{(1),t}$  on stock 2 since  $c_{1,t} < c_{2,t}$ .  
 448 Therefore,  $w_{(1),t} = w_{2,t}$  and  $w_{(2),t} = w_{1,t}$ ;

449 (ii)  $t = k\mathcal{T}$  in panel (a2-e2): The processes evolve towards the rebalancing point  $k\mathcal{T}$ . The relationship  
 450  $w_{(1),t} = w_{2,t}, w_{(2),t} = w_{1,t}$  maintains because there is no rank-swapping between stock 1 and stock  
 451 2;

452 (iii)  $t = k\mathcal{T}^+$  in panels (a3-e3): At the rebalancing point, no active trading is needed as  $w_{(1),t} =$   
 453  $w_{2,t}, w_{(2),t} = w_{1,t}$  for  $i = 1, 2$ , and therefore no divergence (latency cost) or cost from bid-ask  
 454 spread incurred;

455 (iv)  $k\mathcal{T} < t \leq (k+1)\mathcal{T}$  in panels (a4-e4, a5-e5): The processes evolve towards the rebalancing point  
 456  $(k+1)\mathcal{T}$ . However, because of the rank switch in capitalization between stock 1 and 2 during the  
 457 interval, the dollar-valued portfolio for rank and the dollar-valued portfolio for name start diverging,  
 458 i.e.  $w_{(1),t} \neq w_{2,t}, w_{(2),t} \neq w_{1,t}$  and reaches a maximum at the next rebalancing point  $(k+1)\mathcal{T}$   
 459 (panel (d4, d5));

460 (v)  $t = (k+1)\mathcal{T}^+$  in panels (a6-e6): We carry out active trading to rebalancing the portfolio  
 461 such that  $w_{(1),t} = w_{1,t}, w_{(2),t} = w_{2,t}$ . This requires cash reserve to compensate (i) divergence  
 462  $w_{(1),t} + w_{(2),t} - w_{1,t} - w_{2,t}$  (panel (d6)), and (ii) cost from the bid-ask spread (e6);

463 (vi)  $t > (k+1)\mathcal{T}^+$  in panels (a7-e7): the system continues to evolve with  $w_{(1),t} = w_{1,t}, w_{(2),t} = w_{2,t}$ ,  
 464 and the divergence becomes zero.

465 From the detailed analysis above, the need for active trading stems from their rank switching during  
 466 the balance interval. Furthermore, the latency cost is tied to the divergence of total dollar portfolio  
 467 weights between rank space and name space,  $w_{(1),t}^{\text{rank}} + w_{(2),t}^{\text{rank}} - w_{1,t}^{\text{name}} - w_{2,t}^{\text{name}}$ . This divergence  
 468 increases with the interval between the time for rank switching and the time for the subsequent  
 469 rebalancing point, suggesting that decreasing rebalancing intervals  $\mathcal{T}$  might reduce the risk of large  
 470 transaction costs by minimizing latency costs.

471 However, the situation becomes more complex when considering the fluctuating nature of the  
 472 capitalization process. In the scenario where two adjacent capitalization processes frequently switch  
 473 ranks, as shown in Fig. 9, trading too frequently in response to the instantaneous rank changes can  
 474 incur substantial, yet unnecessary costs from bid-ask spread. To illustrate this, we present a similar  
 475 two-particle system where fluctuating capitalization processes cross their paths (Fig. 9(a1-a3)). We  
 476 calculate dollar portfolio weights in name space and rank space according to the aforementioned  
 477 intraday rebalancing strategy, and analyze the divergence of total dollar portfolio weights between rank  
 478 space and name space (Fig. 9(b1-b3)), the cumulative latency costs (Fig. 9(c1-c3)), the cumulative  
 479 costs from bid-ask spread (Fig. 14(d1-d3)), and the cumulative transaction cost (Fig. 9(e1-e3)). We  
 480 consider three scenarios under large, medium, and small rebalancing intervals. Remarkably, our  
 481 findings underscore a return-risk trade-off: frequent trading (short rebalancing interval) yields lower  
 482 divergence and hence lower risk but incurs higher costs from the bid-ask spread, whereas less frequent  
 483 trading (large rebalancing interval) results in higher divergence and risk but lower bid-ask costs.  
 484 Thus, selecting an appropriate rebalancing interval is crucial for minimizing overall transaction costs  
 485 by balancing between latency costs and costs from bid-ask spread. Indeed, we observe a strong  
 486 dependence on the profit and loss (PnL) with different intraday rebalance intervals in our empirical  
 487 analysis (Fig. 14).

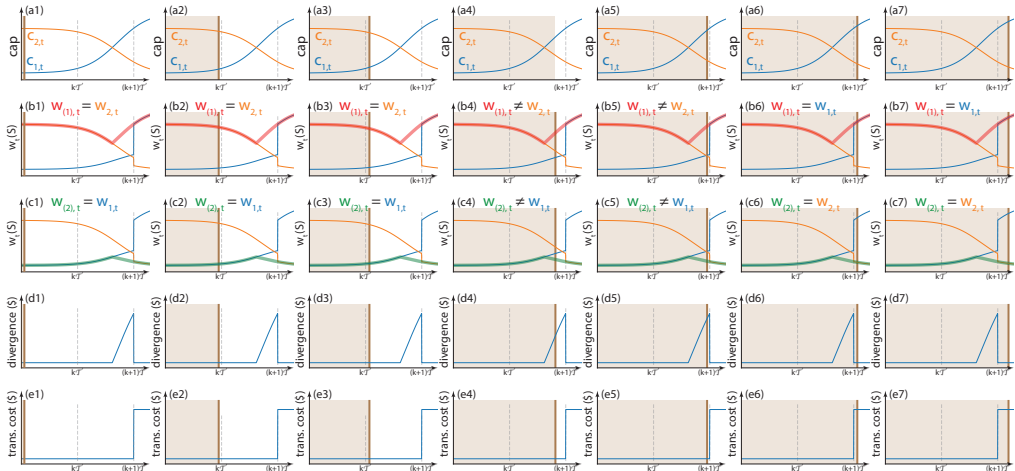


**Figure 8: Schematic for the intraday rebalancing through rank switching of two stocks.** Here, we examine a two-stock system and highlight the critical role of the rank switching. We consider two capitalization processes  $c_{t,1}$  and  $c_{t,2}$  that maintain their ranks during the rebalancing interval  $((k-1)\mathcal{T}, k\mathcal{T}]$  and switch their ranks during  $(k\mathcal{T}, (k+1)\mathcal{T}]$  (panel (a1-a7)). The red lines in panel (b1-b7) and green lines in panel (c1-c7) show the dollar-valued portfolio in rank space  $w_{(1),\tau}$  and  $w_{(2),\tau}$  respectively, where  $w_{(k),t}$  denotes the dollar portfolio weights on the stock that occupies  $k$ -th rank in capitalization. The orange line in panel (b1-b7) and blue line in panel (c1-c7) show the dollar-valued portfolio in name space  $w_{1,\tau}$  and  $w_{2,\tau}$  respectively, where  $w_{i,\tau}$  denotes the dollar portfolio weights on the stock that had  $i$ -th name index. We further calculate and present in panel (d1-d7) the divergence between the total dollar portfolio weights in rank space and in name space, defined as  $w_{(1),t} + w_{(2),t} - w_{1,t} - w_{2,t}$ . Panel (e1-e7) shows the cumulative cost from bid-ask spread arising from the active trading at the rebalancing point.

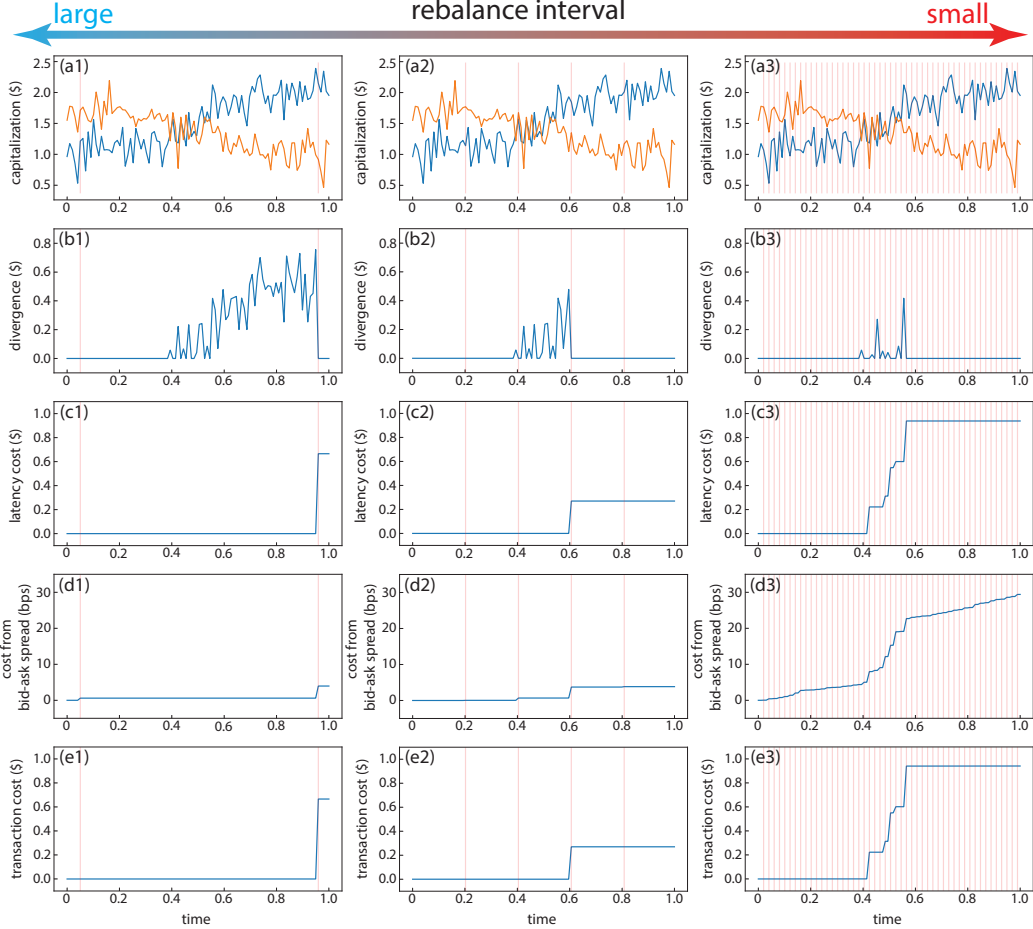


**Figure 9: Transaction cost dependence on the rebalancing interval.** This figure illustrates how transaction costs incurred by intraday rebalancing are influenced by different rebalancing intervals: large (panel (a1-e1)), medium (panel (a2-e2)), and small (panel (a1-a3)). The red vertical lines mark the rebalancing points across all panels. **(a1-a3)** The capitalization processes from two stocks. **(b1-b3)** The divergence between the total dollar portfolio weights in rank space and name space,  $w_{(1),t} + w_{(2),t} - w_{1,t} + w_{2,t}$ . The dollar portfolio weights in rank space  $w_{(1),t}, w_{(2),t}$ , and in name space  $w_{1,t}, w_{2,t}$  are calculated based on capitalization processes in (a) following the intraday rebalancing strategy similar to Fig. 8. The maximum divergence decreases as rebalancing interval increases, aiding risk control. **(c1-c3)** The cumulative latency cost required to compensating divergences at the rebalancing points. Each point of rebalancing incurs a latency cost equal to the divergence between the total dollar portfolio weights in rank space and name space. **(d1-d3)** The cumulative cost from the bid-ask spread due to active trading at each rebalancing point. **(e1-e3)** The cumulative transaction cost. The cumulative transaction costs are the sum of latency costs and transaction costs. The medium rebalancing interval results in the lowest transaction costs while maintaining a manageable divergence, illustrating the importance of choosing an appropriate rebalancing interval.

488 **E Benchmark parametric model**

489 Our parametric model serves as the benchmark for DNNs comparison and follows closely to the  
 490 framework proposed by Avellaneda and Lee[3] and refined by Yeo and Papanicolaou[28]. This model  
 491 applies to both name space and rank space, depending on whether  $x_t^L$  or  $\tilde{x}_t^L$  is chosen as the input.  
 492 We first fit  $x_t^L$  to an OU process  $X_t$  governed by the stochastic differential equation

$$dX_t = \frac{1}{\tau}(\mu - X_t)dt + \sigma dB_t, \quad (\text{E.1})$$

493 where  $\tau$  is the mean-reverting time,  $\mu$  is the long-term average of  $X_t$ ,  $B_t$  is the standard Brownian  
 494 motion, and  $\sigma$  is its volatility. Subsequently, we calculate the trading signal in name space

$$s_{i,t}^{\text{OU}} = \frac{x_{i,t} - \hat{\mu}_i}{\hat{\sigma}_i}, \quad (\text{E.2})$$

495 where  $\hat{\mu}_i, \hat{\sigma}_i$  are the maximum likelihood estimator of  $\mu$  and  $\sigma$ [3] and  $x_{i,t}$  is the terminal cumulative  
 496 residual return at time  $t$ ,

$$x_{i,t} = \sum_{j=1}^L \epsilon_{i,t-L+j}. \quad (\text{E.3})$$

497 We also include the estimated mean-reverting time  $\hat{\tau}$  to effectively filter the trading opportunities[28].  
 498 The details of parameter estimation are presented in the Appendix. We open short/long positions when  
 499 observing large positive/negative signals and close positions when the trading signals mean-revert  
 500 close to zero (schematic in Fig. 10). Following the principle, the portfolio weights in residual space,  
 501  $w_t^{\epsilon|\text{OU,name/rank}}$  become

$$w_{i,t}^{\epsilon|\text{OU,name/rank}} = \begin{cases} -1, & \text{if } w_{i,t-1}^{\epsilon|\text{OU}} = 0, \quad s_{i,t}^{\text{OU}} > c_{\text{thresh-open}}, \quad \hat{\tau}_i < 30 \text{ days} \\ 1, & \text{if } w_{i,t-1}^{\epsilon|\text{OU}} = 0, \quad s_{i,t}^{\text{OU}} < -c_{\text{thresh-open}}, \quad \hat{\tau}_i < 30 \text{ days} \\ 1, & \text{if } w_{i,t-1}^{\epsilon|\text{OU}} = 1, \quad s_{i,t}^{\text{OU}} > c_{\text{thresh-close}}, \quad \hat{\tau}_i < 30 \text{ days} \\ -1, & \text{if } w_{i,t-1}^{\epsilon|\text{OU}} = -1, \quad s_{i,t}^{\text{OU}} > c_{\text{thresh-close}}, \quad \hat{\tau}_i < 30 \text{ days} \\ 0, & \text{otherwise} \end{cases} \quad (\text{E.4})$$

502 For our back-testing, the parameters are set as follows:

$$c_{\text{thresh-open}} = 1.25, \quad c_{\text{thresh-close}} = 0.5, \quad (\text{E.5})$$

503 in accordance with [3, 28]. After calculating  $w_t^{\epsilon|\text{OU,name/rank}}$ , the conversion to portfolio weights in  
 504 equity space,  $w_t^{R|\text{OU,name/rank}}$ , straightforwardly follow the (3.4) in name space

$$w_t^{R|\text{OU,name}} = \Phi_t^T w_t^{\epsilon|\text{OU,name}} \quad (\text{E.6})$$

505 and from (3.8) in rank space,

$$w_t^{R|\text{OU,rank}} = \tilde{\Phi}_t^T w_t^{\epsilon|\text{OU,name}}. \quad (\text{E.7})$$

506 The practical implementation of the parametric model is summarized in Algorithm 2 along with a  
 507 schematic in panel (d1, e1) in Fig. 1.

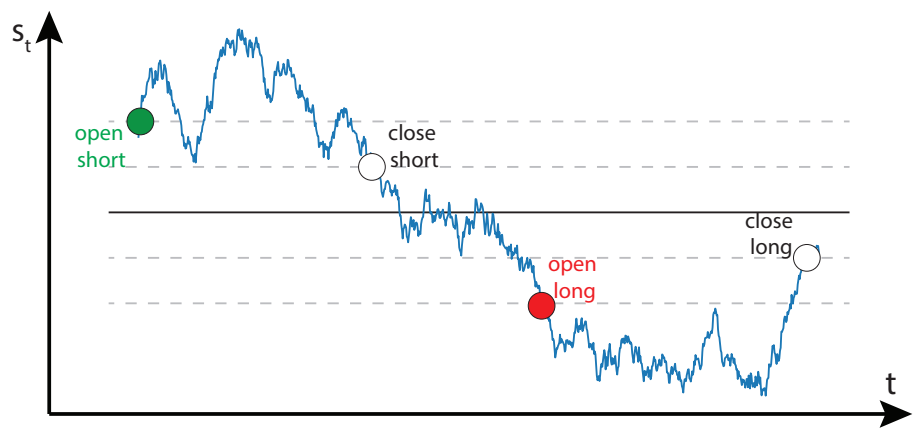


Figure 10: **Schematic for the parametric model.** The blue line shows the trading signal  $s_t$ . We open short/long positions when observing large positive/negative signals and close positions when the trading signals mean-revert to zero.

508 **F Non-parametric analysis on mean-reversion of residual returns**

509 The superior mean-reverting behavior in rank space is further demonstrated by comparing the  
 510 empirical distribution of normalized cumulative residual returns,  $\tilde{x}_t^L$  calculated from name space and  
 511 rank space. We define the normalized cumulative residual returns as follows:

$$\hat{x}_t^L = (\hat{x}_{t-L+1}, \hat{x}_{t-L+2}, \dots, \hat{x}_t), \quad \text{where } \hat{x}_{t-L+\alpha} = \frac{1}{\hat{\sigma}_t^L \sqrt{\alpha}} \sum_{j=1}^{\alpha} \epsilon_{t-L+j} \quad (\text{F.1})$$

512 , where  $\hat{\sigma}_t^L$  is the estimated standard deviation of  $\{\epsilon_{t-L+j}\}_{j=1}^L$ . Suppose the residual returns follow  
 513 uncorrelated, normal distribution, i.e.  $\{\epsilon_{t-L+j}\}_{j=1}^L \sim \mathcal{N}(\mathbf{0}, \mathbf{I}_L)$ , the derived cumulative residual  
 514 returns  $x_t^L$  will follow a standard Brownian motion and the normalized cumulative residual return  
 515 defined in (F.1) will be normally distributed, i.e.  $\hat{x}_{t-L+\alpha} \sim \mathcal{N}(0, 1)$ ,  $\forall \alpha = 1, 2, \dots, L$ . Consequently,  
 516 it will serve as a measure of mean-reversion of the difference in probability density function (p.d.f.)  
 517 between the empirical observations on market and the normal distribution,

$$\text{p.d.f.}(\hat{x}_{t-L+\alpha}) = \frac{1}{\sqrt{2\pi}} \exp\left(-\frac{\hat{x}_{t-L+\alpha}^2}{2}\right), \quad \alpha = 1, 2, \dots, L \quad (\text{F.2})$$

518 The difference is accessed over a series of five-year periods from 1991 to 2022 for both name space  
 519 (Fig. 11(a1-a6)) and rank space (Fig. 11(b1-b6)). A more concentrated distribution of  $\hat{x}_{t-L+\alpha}$  than  
 520 Brownian motion indicates good mean-reverting behavior, especially for large  $\alpha$ . This is particularly  
 521 evident in rank space, where a robust dominance of red color in the heatmaps for large  $\alpha$  regime  
 522 (highlighted in dashed boxes in Fig. 11) underscores the concentrated nature of  $\hat{x}_t^L$  in rank space.  
 523 Such behavior provides critical evidence of a more robust mean-reversion of residual returns in rank  
 524 space. In stark contrast, the similar dominance by red color in name space was evident in 1990s  
 525 (Fig. 11(a1, a2)), but progressively deteriorated since 2000s (Fig. 11(a5-a6)), and finally disappears  
 526 after 2010s (Fig. 11(a5-a6)). This marks the deterioration of the mean-reversion of  $x_t^L$  in name space  
 527 after the 2010s, echoing the failure of profiting from conventional statistical arbitrage strategies after  
 528 2010s.

529 In summary, our non-parametric analysis here demonstrates that the rank space exhibits more robust  
 530 mean-reverting behavior compared to name space, echoing the parametric analysis on mean-reverting  
 531 time in the main text.

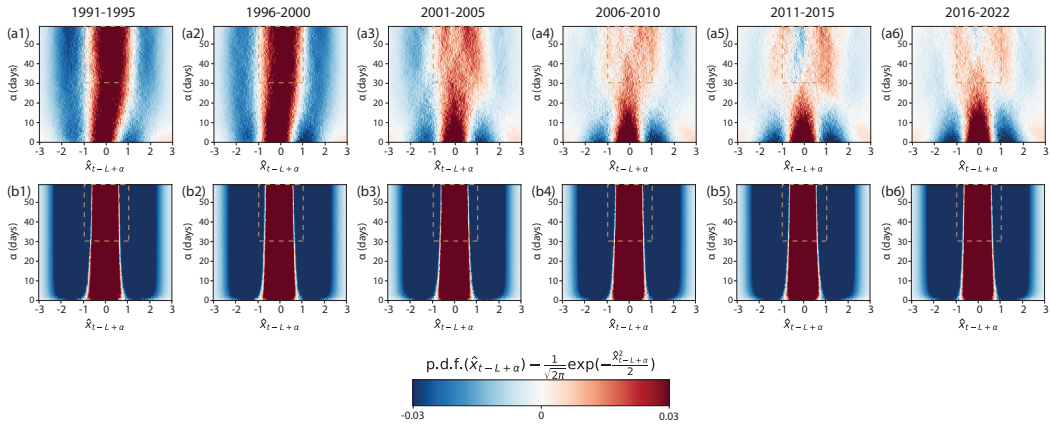


**Figure 11: Empirical distributions of normalized cumulative residual returns: name space versus rank space.** The cumulative residual returns  $x_t^L$  are normalized according to (F.1). This normalization facilitates the conversion of comparisons between trajectories of  $x_t^L$  and Brownian motion into comparisons of the probability density of the empirical distribution of  $\hat{x}_t^L$  against the normal distribution. Consequently, we present the difference between the empirical probability density of  $\hat{x}_t^L$  and standard normal distribution. The empirical probability density of  $\hat{x}_t^L$  is evaluated across a series of five-year periods from 1991 (left) to 2022 (right) in both **(a1-a6)** name space and **(b1-b6)** rank space. The dashed brown box highlights the critical regime where a dominating red color indicates a more concentrated distribution of  $x_{t-L+\alpha}$  for large  $\alpha$ . This concentration signals superior mean-reversion capabilities, particularly evident in rank space throughout the last thirty years. Furthermore, the distribution of  $\hat{x}_t^L$  in name space evolves significantly, indicating a progressively deteriorating mean-reversion after 2010. This echoes the relatively poor performance in our backtesting. The stark contrast in  $\hat{x}_t^L$  supports the strategic advantage of operating in rank space for statistical arbitrage.

532 **G Portfolio performance**

533 **G.1 Annualized return, volatility, and Sharpe ratio**

534 We calculate the annualized return, volatility, and Sharpe ratio derived from the PnL  $V_t$  in Fig. 5. The  
 535 annualized summary statistics without and with transaction costs are presented in Table 1 and Table 2,  
 536 respectively, where we consider corresponding portfolio weights  $w_t^R$  calculated by four scenarios: (i)  
 537 the parametric benchmark model in name space in panel (a), (ii) the parametric benchmark model in  
 538 rank space in panels (b,c), (iii) DNNs in name space in panel (d), and (iv) DNNs in rank space in  
 539 panels (e, f).

year	Name space parametric model			rank space parametric model			name space neural networks			rank space neural networks		
	return	vol	SR	return	vol	SR	return	vol	SR	return	vol	SR
2007	2.87%	0.02	1.38	8.52%	0.04	1.90	-8.37%	0.10	-0.87	79.41%	0.14	5.62
2008	7.42%	0.04	1.70	25.44%	0.06	3.96	-6.98%	0.13	-0.52	239.88%	0.38	6.36
2009	7.01%	0.03	2.02	27.81%	0.08	3.57	3.91%	0.13	0.29	414.09%	0.35	11.72
2010	-0.49%	0.02	-0.24	31.73%	0.05	6.21	-0.02%	0.08	0.00	222.37%	0.19	11.41
2011	1.91%	0.02	0.85	40.14%	0.06	7.12	12.84%	0.08	1.67	126.84%	0.22	5.76
2012	-0.40%	0.02	-0.22	41.06%	0.05	8.20	7.35%	0.07	1.00	162.37%	0.20	8.20
2013	1.19%	0.02	0.70	27.92%	0.05	5.74	8.34%	0.07	1.14	289.73%	0.21	13.96
2014	3.65%	0.02	2.07	43.82%	0.05	8.84	-3.24%	0.07	-0.49	168.89%	0.14	12.07
2015	0.81%	0.02	0.41	41.78%	0.06	7.44	0.71%	0.08	0.09	137.95%	0.19	7.10
2016	2.79%	0.02	1.43	61.86%	0.07	9.51	8.58%	0.10	0.90	293.85%	0.27	11.02
2017	1.56%	0.02	0.93	30.58%	0.04	7.04	9.88%	0.07	1.35	208.30%	0.17	12.10
2018	3.07%	0.02	1.44	27.78%	0.05	5.71	3.67%	0.06	0.60	151.91%	0.19	7.83
2019	4.50%	0.02	2.44	41.42%	0.05	8.39	-6.84%	0.06	-1.07	175.91%	0.20	8.59
2020	1.56%	0.04	0.39	25.06%	0.09	2.89	1.24%	0.09	0.14	307.81%	0.28	10.84
2021	-0.67%	0.02	-0.28	37.60%	0.06	6.21	-2.32%	0.08	-0.30	177.60%	0.25	7.11
2022	1.05%	0.03	0.36	36.79%	0.07	5.53	28.84%	0.09	3.29	146.86%	0.29	5.00
Avg	2.36%	0.02	0.96	34.33%	0.06	6.14	3.60%	0.08	0.45	206.49%	0.23	9.04

Table 1: **Portfolio performance without transaction costs.** The portfolios in rank space consistently outperform their counterparts in name space, both with the parametric model and neural networks. The neural networks improve the portfolio performance in rank space dramatically, in stark contrast with negligible improvements in name space. The contrast echoes with the fact that the neural networks are much more effective in rank space compared to that in name space Fig. 7.

year	Name space parametric model			rank space parametric model			name space neural networks			rank space neural networks		
	return	vol	SR	return	vol	SR	return	vol	SR	return	vol	SR
2007	1.63%	0.02	0.79	-32.51%	0.04	-7.67	-15.51%	0.10	-1.61	26.07%	0.10	2.55
2008	6.02%	0.04	1.38	-43.78%	0.05	-9.58	-14.19%	0.13	-1.06	36.40%	0.18	2.04
2009	5.71%	0.03	1.65	-32.78%	0.04	-8.07	-3.13%	0.13	-0.23	48.97%	0.13	3.67
2010	-1.69%	0.02	-0.82	-32.83%	0.03	-12.68	-7.25%	0.08	-0.91	43.14%	0.10	4.32
2011	0.71%	0.02	0.31	-32.45%	0.03	-12.02	5.10%	0.08	0.66	14.32%	0.10	1.45
2012	-1.52%	0.02	-0.84	-26.53%	0.02	-11.84	-0.20%	0.07	-0.03	20.41%	0.08	2.42
2013	0.02%	0.02	0.01	-25.14%	0.02	-11.16	0.21%	0.07	0.03	52.51%	0.10	5.37
2014	2.45%	0.02	1.39	-22.52%	0.02	-9.74	-10.25%	0.07	-1.55	35.55%	0.07	4.76
2015	-0.31%	0.02	-0.16	-20.12%	0.03	-7.38	-6.89%	0.08	-0.89	22.82%	0.10	2.32
2016	1.65%	0.02	0.85	-17.68%	0.03	-5.45	0.43%	0.10	0.05	56.09%	0.13	4.31
2017	0.36%	0.02	0.22	-21.38%	0.02	-9.28	2.62%	0.07	0.36	49.00%	0.09	5.16
2018	1.86%	0.02	0.87	-28.83%	0.03	-11.45	-4.16%	0.06	-0.68	27.94%	0.10	2.81
2019	3.34%	0.02	1.81	-21.49%	0.02	-8.92	-13.52%	0.06	-2.12	34.13%	0.10	3.38
2020	0.21%	0.04	0.05	-42.12%	0.05	-9.02	-5.62%	0.09	-0.62	56.62%	0.14	4.14
2021	-2.06%	0.02	-0.86	-36.82%	0.03	-13.27	-9.69%	0.08	-1.27	31.14%	0.13	2.47
2022	-0.16%	0.03	-0.06	-33.01%	0.03	-11.71	19.19%	0.09	2.19	15.69%	0.12	1.26
Avg	1.14%	0.02	0.41	-29.37%	0.03	-9.95	-3.93%	0.08	-0.48	35.68%	0.11	3.28

Table 2: **Portfolio performance with transaction costs.** The portfolio performances in rank space degrade dramatically, for both the parametric model and the neural networks. The substantial degradation arises from the substantial costs associated with realizing rank return in continuous time limit through intraday rebalancing. Nevertheless, the portfolio calculated by neural networks in rank space still yields good results, as the significant transaction costs are compensated by the impressive returns and Sharpe ratio in Table 1, column 4. We choose 2 basis points to account for the transaction costs from bid-ask spread.

540 **G.2 Dollar neutrality**

541 We characterize the long or short proportion of the portfolio weights in equity space,  $\sum_{i:w_{i,t}^R > 0} w_{i,t}$   
 542 or  $\sum_{i:w_{i,t}^R < 0} w_{i,t}$  and the dollar neutrality,  $\frac{\sum_i w_{i,t}^R}{\sum_i |w_{i,t}^R|}$ . The results are presented in Fig. 12(a1-d1) and  
 543 Fig. 12(a2-d2), where we consider  $w_t^R$  calculated by four scenarios: (i) the parametric benchmark  
 544 model in name space (Fig. 12(a1, a2)), (ii) DNNs in name space (Fig. 12(b1, b2)), (iii) the parametric  
 545 benchmark model in rank space (Fig. 12(c1, c2)), (iv) DNNs in rank space (Fig. 12(d1, d2)). Notably,  
 546 the long or short proportion of  $w_t^R$  by neural networks (Fig. 12(b1, d1)) is much more volatile than  
 547 those by the parametric model (Fig. 12(a1, c1)), as a result of flexible leverage adopted by neural  
 548 networks. However, the dollar neutrality is satisfied on average thanks to the market neutrality of the  
 549 portfolios.

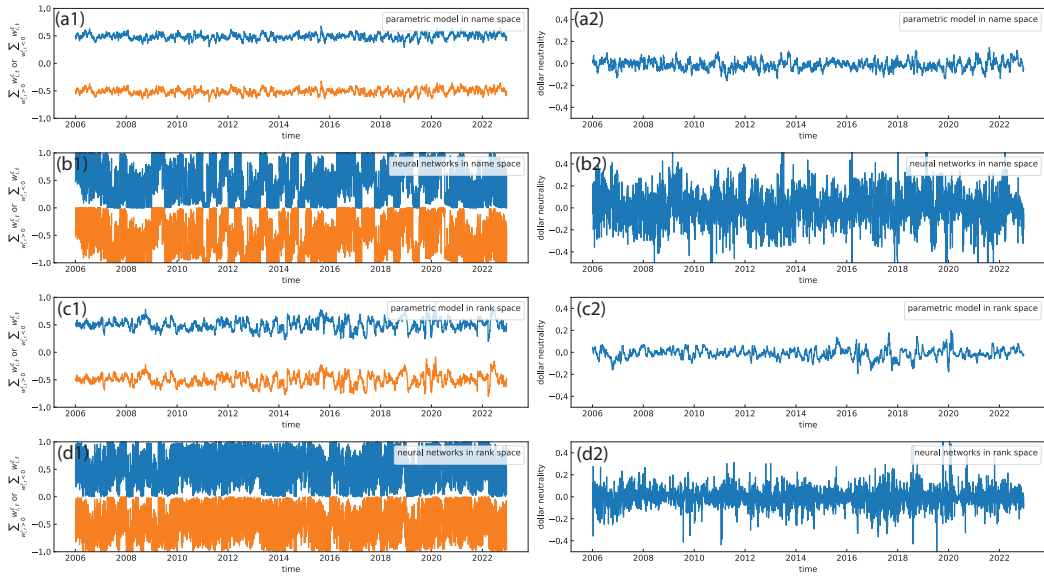


Figure 12: **Portfolio weights in residual return and dollar neutrality.** (a1-d1) The temporal dependence of average long/short portfolio weights in residual space,  $\sum_{i:w_{i,t}^e > 0} w_{i,t}^e$  and  $\sum_{i:w_{i,t}^e < 0} w_{i,t}^e$ .  
 (a2-d2) The deviation from dollar neutrality measured by  $\frac{\sum_i w_{i,t}^R}{\sum_i |w_{i,t}^R|}$ . We consider four scenarios:  
 (a1-a2) parametric model in name space; (b1-b2) neural networks in name space; (c1-c2) parametric  
 model in rank space; (d1-d2) neural networks in rank space.

550 **G.3 Dependence on transaction costs**

551 We present the sensitivity of portfolio performance to transaction costs. We show the PnL with  
 552 different transaction cost factor  $\eta$  in Fig. 13(a) and the corresponding Sharpe ratio in Fig. 13. The  
 553 current strategy shows significant sensitivity to the transaction cost factor and stops to profit with  
 554  $\eta = 5$  basis points. A more effective strategy to realize return in rank space  $\tilde{r}_t$  will help the strategy  
 555 more immune to transaction costs.

556 **G.4 A characteristic time between rank switching**

557 The rebalancing interval,  $\mathcal{T}$ , turns out to be a crucial parameter for statistical arbitrage portfolios  
 558 in rank space. To demonstrate, we present the calculated PnL with varying rebalancing intervals  
 559 in Fig. 14(a), where the portfolio weights are calculated from the neural networks in rank space.  
 560 The associated average Sharpe ratio and terminal PnL as a function of the rebalancing interval are  
 561 summarized in Fig. 14(b), with both peaking at 225 minutes.

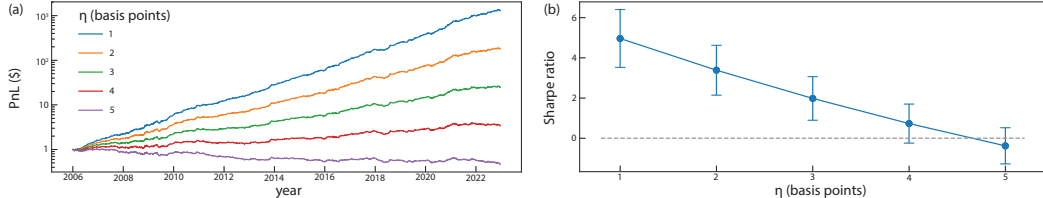


Figure 13: **PnL dependence on transaction cost factor  $\eta$ .** **(a)** The PnL with varying levels of the transaction cost factor  $\eta$ . The underlying portfolio weights are derived from the neural networks in rank space. **(b)** The average Sharpe ratio from 2006 to 2022 at different values of  $\eta$  derived from (a). The strategy stops to profit with 5 basis points transaction costs due to substantial costs associated with realizing rank returns in continuous time limit. The significant change in Sharpe ratio under varying transaction costs underscores the strategy's sensitivity to transaction costs and motivates ongoing improvements in "trading ranks".

562 Here, we delve into the rationale behind the optimal 225-minute interval, starting with an examination  
 563 of two proximate capitalization processes modeled as Brownian motions,  $c_{1,t}$  and  $c_{2,t}$  (Fig. 14(c)).  
 564 Given that transaction costs from intraday rebalancing primarily arise from rank swaps in capital-  
 565 ization (section 2.3), we measure the cumulative time  $\Lambda(t)$  that the capitalization processes cross  
 566 (Fig. 14(c), red line),

$$\Lambda(t) = \lim_{\delta \downarrow 0} \int_0^t \mathbf{1}_{\{|c_{1,\tau} - c_{2,\tau}| \leq \delta\}} d\tau \quad (\text{G.1})$$

567 The rank-swapping interval  $\lambda$  is defined as the time between the cross of capitalization processes,  
 568 or equivalently, the increments of  $\Lambda(t)$ . This classical interacting Brownian system features two  
 569 characteristic regimes: (i) the idle regime, where the two capitalization processes are distant, main-  
 570 taining constant  $\Lambda(t)$  with prolonged  $\lambda$ ; (ii) the collision regime (highlighted in brown shaded area in  
 571 Fig. 14(c)), where the two capitalization processes stay close, leading to rapid increases in  $\Lambda(t)$  and  
 572 short  $\lambda$ . We show the empirical distribution of  $\lambda$  on real market in Fig. 14(d), where the small  $\lambda$  values  
 573 arise from the collision regime and larger  $\lambda$  values from the idle regime, following approximately  
 574 an exponential distribution as a typical signature for standard Brownian particle systems. The 225  
 575 minutes is situated at the intersection of the two regimes, establishing it as a characteristic time for  
 576 rank switching.

577 In the detailed analysis of the intraday rebalancing in (3.14) and Fig. 9, the transaction costs arise  
 578 from (i) latency costs due to delayed reactions post-rank-swapping, and (ii) costs from bid-ask spreads  
 579 incurred during active trading. For the collision regime in Fig. 14(c), it is preferable to delay trading  
 580 to minimize bid-ask spread costs. Conversely, in the idle regime, immediate trading is preferable to  
 581 reduce latency costs. The 225-minute interval effectively differentiates these regimes, thus optimizing  
 582 overall transaction costs.

583 The discussion above highlights the challenge in trading ranks – discerning between the collision  
 584 and idle regimes and trading at their intersection. Our current intraday rebalancing approach crudely  
 585 harnesses average behavior of U.S. equity market, and leaves considerable scope for enhancement  
 586 that we will follow up on in subsequent research papers.

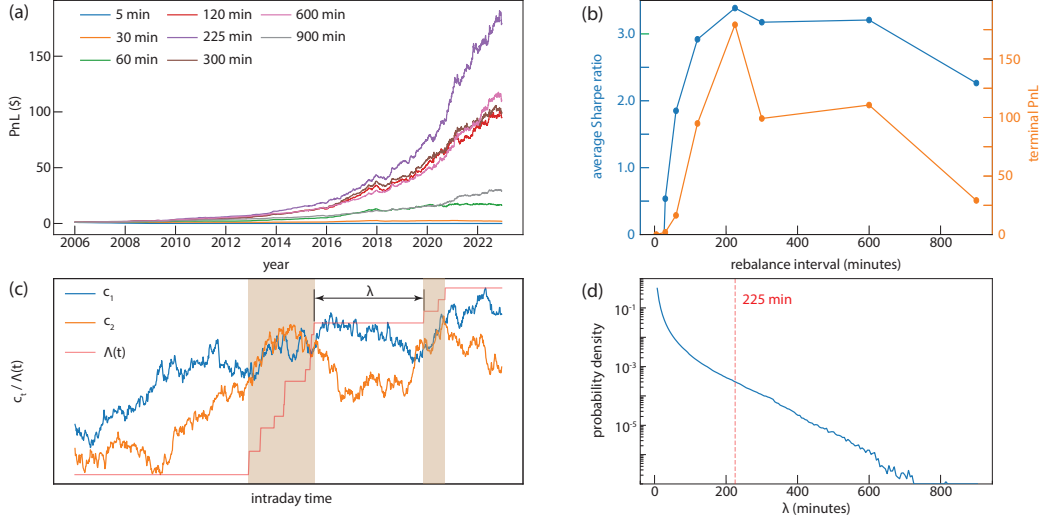


**Figure 14: PnL dependence on rebalancing interval and characteristic rank-swapping time.** **(a)** The PnL across various intraday rebalancing intervals  $\mathcal{T}$  to realize the rank return in continuous time limit  $\tilde{r}_t$ . The underlying portfolio weights are derived from the neural networks in rank space. **(b)** Averaged Sharpe ratio between 2006 and 2022 and the terminal PnL as functions of rebalance intervals from (a). Both metrics peak at  $\mathcal{T} = 225$  minutes. **(c)** Schematic representation of two capitalization processes,  $c_1$  and  $c_2$ . The  $\Lambda(t)$  measures the cumulative time that the capitalization processes  $c_1$  and  $c_2$  cross. Rank switching time  $\lambda$  is the interval between the increments in local time. This stochastic system has two characteristic regimes: (i) the idle regime, where the two capitalization processes are distant, maintaining constant  $\Lambda(t)$  with prolonged  $\lambda$ ; (ii) the collision regime (highlighted in brown shaded area in Fig. 14(c)), where the two capitalization processes stay close, leading to rapid increases in  $\Lambda(t)$  and short  $\lambda$ . **(e)** The empirical distributions of rank-swapping time  $\tau$  based on the intraday market data. Low (high)  $\lambda$  arises from the "idle" ("collision") regime. The red dashed line marks the optimal rebalancing interval,  $\mathcal{T} = 225$  minutes, positioned at the intersection between the idle and collision regimes, suggesting it is a balanced choice for minimizing transaction costs while responding effectively with rank-swapping events.

587 **References**

- 588 [1] Fernando Acero, Parisa Zehtabi, Nicolas Marchesotti, Michael Cashmore, Daniele Magazzeni,  
589 and Manuela Veloso. Deep reinforcement learning and mean-variance strategies for responsible  
590 portfolio optimization. *arXiv:2403.16667*, 2024.
- 591 [2] Dogu Araci. Finbert: Financial sentiment analysis with pre-trained language models. arxiv  
592 2019. *arXiv preprint arXiv:1908.10063*, 2019.
- 593 [3] Marco Avellaneda and Jeong-Hyun Lee. Statistical arbitrage in the US equities market. *Quanti-  
594 tative Finance*, 10(7):761–782, 2010.
- 595 [4] Marco Avellaneda, Brian Healy, Andrew Papanicolaou, and George Papanicolaou. Principal  
596 eigenportfolios for US equities. *SIAM Journal on Financial Mathematics*, 13(3):702–744, 2022.
- 597 [5] Jimmy Lei Ba, Jamie Ryan Kiros, and Geoffrey E Hinton. Layer normalization.  
598 *arXiv:1607.06450*, 2016.
- 599 [6] Adrian D Banner and Raouf Ghomrasni. Local times of ranked continuous semimartingales.  
600 *Stochastic Processes and their Applications*, 118(7):1244–1253, 2008.
- 601 [7] Adrian D Banner, Robert Fernholz, and Ioannis Karatzas. Atlas models of equity markets.  
602 *Annals of applied probability*, 15(4):2296–2330, 2005.
- 603 [8] Howard C Berg. *Random walks in biology*. Princeton University Press, 1993.
- 604 [9] Jean-Philippe Bouchaud and Marc Potters. Financial applications of random matrix theory: a  
605 short review. *arXiv preprint arXiv:0910.1205*, 2009.
- 606 [10] Álvaro Cartea, Sebastian Jaimungal, and José Penalva. *Algorithmic and high-frequency trading*.  
607 Cambridge University Press, 2015.
- 608 [11] E Robert Fernholz and E Robert Fernholz. *Stochastic portfolio theory*. Springer, 2002.
- 609 [12] Cesar Garcia-Diaz. Sociophysics: A physicist’s modeling of psycho-political phenomena  
610 (understanding complex systems), 2013.
- 611 [13] Shihao Gu, Bryan Kelly, and Dacheng Xiu. Empirical asset pricing via machine learning. *The  
612 Review of Financial Studies*, 33(5):2223–2273, 2020.
- 613 [14] Jorge Guijarro-Ordonez, Markus Pelger, and Greg Zanotti. Deep learning statistical arbitrage.  
614 *arXiv:2106.04028*, 2021.
- 615 [15] Kaiming He, Xiangyu Zhang, Shaoqing Ren, and Jian Sun. Deep residual learning for image  
616 recognition. *Proceedings of the IEEE conference on computer vision and pattern recognition*,  
617 pages 770–778, 2016.
- 618 [16] Brian Healy, Y.-F. Li, A Papanicolaou, and P Papanicolaou. The data stabilizing transformation  
619 from named to ranked equity returns. *working paper*, 2025.
- 620 [17] Blanka Horvath, Aitor Muguruza, and Mehdi Tomas. Deep learning volatility: a deep neural  
621 network perspective on pricing and calibration in (rough) volatility models. *Quantitative  
622 Finance*, 21(1):11–27, 2021.
- 623 [18] Tomoyuki Ichiba, Vassilios Papathanakos, Adrian Banner, Ioannis Karatzas, and Robert Fern-  
624 holz. Hybrid atlas models. *Annals of applied probability*, 21(2):609–644, 2011.
- 625 [19] Taewook Kim and Ha Young Kim. Optimizing the pairs-trading strategy using deep reinforce-  
626 ment learning with trading and stop-loss boundaries. *Complexity*, 2019(1):3582516, 2019.
- 627 [20] Tim Siu-tang Leung and Xin Li. *Optimal mean reversion trading: Mathematical analysis and  
628 practical applications*, volume 1. World Scientific, 2015.
- 629 [21] Gerald D Mahan. *Many-particle physics*. Springer Science & Business Media, 2013.
- 630 [22] John M Mulvey, Yifan Sun, Mengdi Wang, and Jing Ye. Optimizing a portfolio of mean-  
631 reverting assets with transaction costs via a feedforward neural network. *Quantitative Finance*,  
632 20(8):1239–1261, 2020.
- 633 [23] Szilárd Pafka and Imre Kondor. Noisy covariance matrices and portfolio optimization ii. *Physica  
634 A: Statistical Mechanics and its Applications*, 319:487–494, 2003.
- 635 [24] Maziar Raissi, Paris Perdikaris, and George E Karniadakis. Physics-informed neural networks:  
636 A deep learning framework for solving forward and inverse problems involving nonlinear partial  
637 differential equations. *Journal of Computational physics*, 378:686–707, 2019.

- 638 [25] Agnès Tourin and Raphael Yan. Dynamic pairs trading using the stochastic control approach.  
639 *Journal of Economic Dynamics and Control*, 37(10):1972–1981, 2013.
- 640 [26] Dmitry Ulyanov, Andrea Vedaldi, and Victor Lempitsky. Instance normalization: The missing  
641 ingredient for fast stylization. *arXiv:1607.08022*, 2016.
- 642 [27] Ashish Vaswani, Noam Shazeer, Niki Parmar, Jakob Uszkoreit, Llion Jones, Aidan N Gomez,  
643 Łukasz Kaiser, and Illia Polosukhin. Attention is all you need. *Advances in neural information  
644 processing systems*, 30, 2017.
- 645 [28] Joongyeub Yeo and George Papanicolaou. Risk control of mean-reversion time in statistical  
646 arbitrage. *Risk and Decision Analysis*, 6(4):263–290, 2017.
- 647 [29] Jiongmin Yong and Xun Yu Zhou. *Stochastic controls: Hamiltonian systems and HJB equations*,  
648 volume 43. Springer Science & Business Media, 2012.

## 649 NeurIPS Paper Checklist

650 The checklist is designed to encourage best practices for responsible machine learning research,  
651 addressing issues of reproducibility, transparency, research ethics, and societal impact. Do not remove  
652 the checklist: **The papers not including the checklist will be desk rejected.** The checklist should  
653 follow the references and follow the (optional) supplemental material. The checklist does NOT count  
654 towards the page limit.

655 Please read the checklist guidelines carefully for information on how to answer these questions. For  
656 each question in the checklist:

- 657 • You should answer [Yes] , [No] , or [NA] .
- 658 • [NA] means either that the question is Not Applicable for that particular paper or the  
659 relevant information is Not Available.
- 660 • Please provide a short (1–2 sentence) justification right after your answer (even for NA).

661 **The checklist answers are an integral part of your paper submission.** They are visible to the  
662 reviewers, area chairs, senior area chairs, and ethics reviewers. You will be asked to also include it  
663 (after eventual revisions) with the final version of your paper, and its final version will be published  
664 with the paper.

665 The reviewers of your paper will be asked to use the checklist as one of the factors in their evaluation.  
666 While "[Yes]" is generally preferable to "[No]", it is perfectly acceptable to answer "[No]" provided a  
667 proper justification is given (e.g., "error bars are not reported because it would be too computationally  
668 expensive" or "we were unable to find the license for the dataset we used"). In general, answering  
669 "[No]" or "[NA]" is not grounds for rejection. While the questions are phrased in a binary way, we  
670 acknowledge that the true answer is often more nuanced, so please just use your best judgment and  
671 write a justification to elaborate. All supporting evidence can appear either in the main paper or the  
672 supplemental material, provided in Appendix. If you answer [Yes] to a question, in the justification  
673 please point to the section(s) where related material for the question can be found.

674 **IMPORTANT**, please:

- 675 • **Delete this instruction block, but keep the section heading “NeurIPS paper checklist”**,
- 676 • **Keep the checklist subsection headings, questions/answers and guidelines below.**
- 677 • **Do not modify the questions and only use the provided macros for your answers.**

### 678 1. Claims

679 Question: Do the main claims made in the abstract and introduction accurately reflect the  
680 paper’s contributions and scope?

681 Answer: [Yes]

682 Justification: The main claims made in the abstract and introduction accurately reflect the  
683 paper’s contributions and scope. We claim that (1) operating statistical arbitrage in rank  
684 space significantly improves performance over name space when using deep neural networks  
685 (DNNs), and (2) this improvement is attributed to the more structured market dynamics  
686 and enhanced mean-reversion properties in rank space. These claims are systematically  
687 validated through empirical backtesting on U.S. equities from 2007 to 2022, detailed ablation  
688 studies, and analysis of the learned neural network behaviors. The paper remains focused  
689 on demonstrating these two core contributions without over-claiming broader applicability  
690 beyond the presented setup.

691 Guidelines:

- 692 • The answer NA means that the abstract and introduction do not include the claims  
693 made in the paper.
- 694 • The abstract and/or introduction should clearly state the claims made, including the  
695 contributions made in the paper and important assumptions and limitations. A No or  
696 NA answer to this question will not be perceived well by the reviewers.
- 697 • The claims made should match theoretical and experimental results, and reflect how  
698 much the results can be expected to generalize to other settings.

- 699           • It is fine to include aspirational goals as motivation as long as it is clear that these goals  
700           are not attained by the paper.

701           **2. Limitations**

702           Question: Does the paper discuss the limitations of the work performed by the authors?

703           Answer: [Yes]

704           Justification: The paper explicitly discusses the limitations of the work in the *limitations*  
705           and *discussion* section. We highlight that the current strategy is sensitive to transaction  
706           costs due to frequent intraday rebalancing required to realize rank returns, which may  
707           limit its immediate practicality in less liquid markets. We also provide the framework for  
708           future optimization of execution strategies to address this limitation. Additionally, while we  
709           demonstrate our method in financial markets, we recognize that broader generalization to  
710           other many-particle systems is suggested but not empirically validated in this work.

711           Guidelines:

- 712           • The answer NA means that the paper has no limitation while the answer No means that  
713           the paper has limitations, but those are not discussed in the paper.
- 714           • The authors are encouraged to create a separate "Limitations" section in their paper.
- 715           • The paper should point out any strong assumptions and how robust the results are to  
716           violations of these assumptions (e.g., independence assumptions, noiseless settings,  
717           model well-specification, asymptotic approximations only holding locally). The authors  
718           should reflect on how these assumptions might be violated in practice and what the  
719           implications would be.
- 720           • The authors should reflect on the scope of the claims made, e.g., if the approach was  
721           only tested on a few datasets or with a few runs. In general, empirical results often  
722           depend on implicit assumptions, which should be articulated.
- 723           • The authors should reflect on the factors that influence the performance of the approach.  
724           For example, a facial recognition algorithm may perform poorly when image resolution  
725           is low or images are taken in low lighting. Or a speech-to-text system might not be  
726           used reliably to provide closed captions for online lectures because it fails to handle  
727           technical jargon.
- 728           • The authors should discuss the computational efficiency of the proposed algorithms  
729           and how they scale with dataset size.
- 730           • If applicable, the authors should discuss possible limitations of their approach to  
731           address problems of privacy and fairness.
- 732           • While the authors might fear that complete honesty about limitations might be used by  
733           reviewers as grounds for rejection, a worse outcome might be that reviewers discover  
734           limitations that aren't acknowledged in the paper. The authors should use their best  
735           judgment and recognize that individual actions in favor of transparency play an impor-  
736           tant role in developing norms that preserve the integrity of the community. Reviewers  
737           will be specifically instructed to not penalize honesty concerning limitations.

738           **3. Theory Assumptions and Proofs**

739           Question: For each theoretical result, does the paper provide the full set of assumptions and  
740           a complete (and correct) proof?

741           Answer: [Yes]

742           Justification: For each theoretical result, we provide the full set of assumptions and complete  
743           proofs in the Appendix. In particular, we include (i) a detailed proof of the market neutrality  
744           property of the constructed portfolios under the given market decomposition framework,  
745           (ii) a hybrid-Atlas model that motivates operating statistical arbitrage in rank space. All  
746           mathematical arguments are presented carefully, and the proofs are fully self-contained.

747           Guidelines:

- 748           • The answer NA means that the paper does not include theoretical results.
- 749           • All the theorems, formulas, and proofs in the paper should be numbered and cross-  
750           referenced.
- 751           • All assumptions should be clearly stated or referenced in the statement of any theorems.

- 752           • The proofs can either appear in the main paper or the supplemental material, but if  
 753           they appear in the supplemental material, the authors are encouraged to provide a short  
 754           proof sketch to provide intuition.  
 755           • Inversely, any informal proof provided in the core of the paper should be complemented  
 756           by formal proofs provided in Appendix or supplemental material.  
 757           • Theorems and Lemmas that the proof relies upon should be properly referenced.

758          **4. Experimental Result Reproducibility**

759          Question: Does the paper fully disclose all the information needed to reproduce the main ex-  
 760          perimental results of the paper to the extent that it affects the main claims and/or conclusions  
 761          of the paper (regardless of whether the code and data are provided or not)?

762          Answer: [Yes]

763          Justification: We provide full disclosure of the information needed to reproduce the main  
 764          experimental results. Detailed pseudocode for all key algorithms is included in the Appendix.  
 765          In addition, we have uploaded all Python code necessary for calculating the results to a  
 766          public GitHub repository. However, the financial market data used in this study cannot be  
 767          shared publicly: the daily security data are sourced from CRSP, and the high-frequency  
 768          intraday data are sourced from Polygon.io, both of which are under licensing agreements that  
 769          prohibit redistribution. Despite this, we provide sufficient algorithmic and implementation  
 770          details for independent reproduction using equivalent market datasets.

771          Guidelines:

- 772           • The answer NA means that the paper does not include experiments.
- 773           • If the paper includes experiments, a No answer to this question will not be perceived  
 774           well by the reviewers: Making the paper reproducible is important, regardless of  
 775           whether the code and data are provided or not.
- 776           • If the contribution is a dataset and/or model, the authors should describe the steps taken  
 777           to make their results reproducible or verifiable.
- 778           • Depending on the contribution, reproducibility can be accomplished in various ways.  
 779           For example, if the contribution is a novel architecture, describing the architecture fully  
 780           might suffice, or if the contribution is a specific model and empirical evaluation, it may  
 781           be necessary to either make it possible for others to replicate the model with the same  
 782           dataset, or provide access to the model. In general, releasing code and data is often  
 783           one good way to accomplish this, but reproducibility can also be provided via detailed  
 784           instructions for how to replicate the results, access to a hosted model (e.g., in the case  
 785           of a large language model), releasing of a model checkpoint, or other means that are  
 786           appropriate to the research performed.
- 787           • While NeurIPS does not require releasing code, the conference does require all submis-  
 788           sions to provide some reasonable avenue for reproducibility, which may depend on the  
 789           nature of the contribution. For example
  - 790               (a) If the contribution is primarily a new algorithm, the paper should make it clear how  
 791               to reproduce that algorithm.
  - 792               (b) If the contribution is primarily a new model architecture, the paper should describe  
 793               the architecture clearly and fully.
  - 794               (c) If the contribution is a new model (e.g., a large language model), then there should  
 795               either be a way to access this model for reproducing the results or a way to reproduce  
 796               the model (e.g., with an open-source dataset or instructions for how to construct  
 797               the dataset).
  - 798               (d) We recognize that reproducibility may be tricky in some cases, in which case  
 799               authors are welcome to describe the particular way they provide for reproducibility.  
 800               In the case of closed-source models, it may be that access to the model is limited in  
 801               some way (e.g., to registered users), but it should be possible for other researchers  
 802               to have some path to reproducing or verifying the results.

803          **5. Open access to data and code**

804          Question: Does the paper provide open access to the data and code, with sufficient instruc-  
 805          tions to faithfully reproduce the main experimental results, as described in supplemental  
 806          material?

807 Answer: [Yes]

808 Justification: We provide open access to the full Python code necessary to reproduce the main  
809 experimental results on GitHub repository, along with detailed instructions and pseudocode  
810 in the supplemental material. However, we cannot provide open access to the data due to  
811 licensing restrictions: the daily security data are sourced from CRSP and the high-frequency  
812 intraday data from Polygon.io, both of which are proprietary and not publicly distributable.  
813 Despite this, all necessary procedures and implementation details are disclosed to enable  
814 faithful reproduction using equivalent datasets.

815 Guidelines:

- The answer NA means that paper does not include experiments requiring code.
- Please see the NeurIPS code and data submission guidelines (<https://nips.cc/public/guides/CodeSubmissionPolicy>) for more details.
- While we encourage the release of code and data, we understand that this might not be possible, so “No” is an acceptable answer. Papers cannot be rejected simply for not including code, unless this is central to the contribution (e.g., for a new open-source benchmark).
- The instructions should contain the exact command and environment needed to run to reproduce the results. See the NeurIPS code and data submission guidelines (<https://nips.cc/public/guides/CodeSubmissionPolicy>) for more details.
- The authors should provide instructions on data access and preparation, including how to access the raw data, preprocessed data, intermediate data, and generated data, etc.
- The authors should provide scripts to reproduce all experimental results for the new proposed method and baselines. If only a subset of experiments are reproducible, they should state which ones are omitted from the script and why.
- At submission time, to preserve anonymity, the authors should release anonymized versions (if applicable).
- Providing as much information as possible in supplemental material (appended to the paper) is recommended, but including URLs to data and code is permitted.

## 835 6. Experimental Setting/Details

836 Question: Does the paper specify all the training and test details (e.g., data splits, hyper-  
837 parameters, how they were chosen, type of optimizer, etc.) necessary to understand the  
838 results?

839 Answer: [Yes]

840 Justification: We provide all necessary training and testing details. The pseudocode in  
841 the Appendix outlines the complete experimental workflow, including data preparation,  
842 model training, and evaluation. We also specify the full architecture of the neural network  
843 in the appendix, including convolutional and transformer layers, and describe the training  
844 procedure, including input features, objective function (mean-variance optimization), and  
845 training window sizes. Hyperparameters such as the number of channels, kernel sizes,  
846 number of attention heads, and dropout rates are explicitly stated. Our provided pseudocode  
847 and implementation details allow faithful reproduction.

848 Guidelines:

- The answer NA means that the paper does not include experiments.
- The experimental setting should be presented in the core of the paper to a level of detail  
that is necessary to appreciate the results and make sense of them.
- The full details can be provided either with the code, in Appendix, or as supplemental  
material.

## 854 7. Experiment Statistical Significance

855 Question: Does the paper report error bars suitably and correctly defined or other appropriate  
856 information about the statistical significance of the experiments?

857 Answer: [NA]

858 Justification: We report performance using average annual returns and Sharpe ratios across  
859 multiple years (2007–2022), with detailed year-by-year statistics provided in the Appendix.

860 Since our experiments are based on real historical market data rather than simulations,  
861 traditional error bars or confidence intervals over repeated trials are not applicable. Instead,  
862 we present the variability of results across different years to convey the robustness and  
863 statistical significance of our findings.

864 Guidelines:

- 865 • The answer NA means that the paper does not include experiments.
- 866 • The authors should answer "Yes" if the results are accompanied by error bars, confi-  
867 dence intervals, or statistical significance tests, at least for the experiments that support  
868 the main claims of the paper.
- 869 • The factors of variability that the error bars are capturing should be clearly stated (for  
870 example, train/test split, initialization, random drawing of some parameter, or overall  
871 run with given experimental conditions).
- 872 • The method for calculating the error bars should be explained (closed form formula,  
873 call to a library function, bootstrap, etc.)
- 874 • The assumptions made should be given (e.g., Normally distributed errors).
- 875 • It should be clear whether the error bar is the standard deviation or the standard error  
876 of the mean.
- 877 • It is OK to report 1-sigma error bars, but one should state it. The authors should  
878 preferably report a 2-sigma error bar than state that they have a 96% CI, if the hypothesis  
879 of Normality of errors is not verified.
- 880 • For asymmetric distributions, the authors should be careful not to show in tables or  
881 figures symmetric error bars that would yield results that are out of range (e.g. negative  
882 error rates).
- 883 • If error bars are reported in tables or plots, The authors should explain in the text how  
884 they were calculated and reference the corresponding figures or tables in the text.

## 885 8. Experiments Compute Resources

886 Question: For each experiment, does the paper provide sufficient information on the com-  
887 puter resources (type of compute workers, memory, time of execution) needed to reproduce  
888 the experiments?

889 Answer: [Yes]

890 Justification: We provide sufficient information on the computational resources used in the  
891 Appendix. We specify the hardware configuration, including the type of GPU and CPU,  
892 memory capacity, and details of the training process. This information enables readers to  
893 estimate the computational requirements needed to reproduce the experiments.

894 Guidelines:

- 895 • The answer NA means that the paper does not include experiments.
- 896 • The paper should indicate the type of compute workers CPU or GPU, internal cluster,  
897 or cloud provider, including relevant memory and storage.
- 898 • The paper should provide the amount of compute required for each of the individual  
899 experimental runs as well as estimate the total compute.
- 900 • The paper should disclose whether the full research project required more compute  
901 than the experiments reported in the paper (e.g., preliminary or failed experiments that  
902 didn't make it into the paper).

## 903 9. Code Of Ethics

904 Question: Does the research conducted in the paper conform, in every respect, with the  
905 NeurIPS Code of Ethics <https://neurips.cc/public/EthicsGuidelines>?

906 Answer: [Yes]

907 Justification: The research presented in the paper fully conforms to the NeurIPS Code  
908 of Ethics. Our work involves only publicly available financial market data (subject to  
909 standard licensing restrictions) and does not involve human subjects, private information, or  
910 sensitive demographic attributes. We adhere to principles of transparency, reproducibility,  
911 and responsible reporting throughout the paper.

912 Guidelines:

- 913           • The answer NA means that the authors have not reviewed the NeurIPS Code of Ethics.  
 914           • If the authors answer No, they should explain the special circumstances that require a  
 915            deviation from the Code of Ethics.  
 916           • The authors should make sure to preserve anonymity (e.g., if there is a special consid-  
 917            eration due to laws or regulations in their jurisdiction).

## 918           10. Broader Impacts

919           Question: Does the paper discuss both potential positive societal impacts and negative  
 920           societal impacts of the work performed?

921           Answer: [Yes]

922           Justification: Our work introduces a rank-based representation of market dynamics that im-  
 923           proves the learning efficiency of deep neural networks in noisy environments, with potential  
 924           applications beyond finance to complex systems in physics, biology, and social science. By  
 925           providing a more structured and stable modeling framework, this approach may facilitate  
 926           new insights into the behavior of many-particle systems. However, in financial contexts,  
 927           high-frequency statistical arbitrage strategies could contribute to liquidity fragmentation  
 928           or increase market volatility if deployed without appropriate safeguards. Our method is  
 929           also sensitive to transaction costs, which may limit its accessibility to participants with  
 930           unequal technological resources. We encourage future research to explore both beneficial  
 931           applications and responsible deployment of rank-based learning methods.

932           Guidelines:

- 933           • The answer NA means that there is no societal impact of the work performed.  
 934           • If the authors answer NA or No, they should explain why their work has no societal  
 935            impact or why the paper does not address societal impact.  
 936           • Examples of negative societal impacts include potential malicious or unintended uses  
 937           (e.g., disinformation, generating fake profiles, surveillance), fairness considerations  
 938           (e.g., deployment of technologies that could make decisions that unfairly impact specific  
 939           groups), privacy considerations, and security considerations.  
 940           • The conference expects that many papers will be foundational research and not tied  
 941           to particular applications, let alone deployments. However, if there is a direct path to  
 942           any negative applications, the authors should point it out. For example, it is legitimate  
 943           to point out that an improvement in the quality of generative models could be used to  
 944           generate deepfakes for disinformation. On the other hand, it is not needed to point out  
 945           that a generic algorithm for optimizing neural networks could enable people to train  
 946           models that generate Deepfakes faster.  
 947           • The authors should consider possible harms that could arise when the technology is  
 948           being used as intended and functioning correctly, harms that could arise when the  
 949           technology is being used as intended but gives incorrect results, and harms following  
 950           from (intentional or unintentional) misuse of the technology.  
 951           • If there are negative societal impacts, the authors could also discuss possible mitigation  
 952           strategies (e.g., gated release of models, providing defenses in addition to attacks,  
 953           mechanisms for monitoring misuse, mechanisms to monitor how a system learns from  
 954           feedback over time, improving the efficiency and accessibility of ML).

## 955           11. Safeguards

956           Question: Does the paper describe safeguards that have been put in place for responsible  
 957           release of data or models that have a high risk for misuse (e.g., pretrained language models,  
 958           image generators, or scraped datasets)?

959           Answer: [NA]

960           Justification: Our work does not involve the release of pretrained models, scraped datasets,  
 961           or generative models that carry a high risk of misuse. The models we develop are applied  
 962           to historical financial market data under standard licensing restrictions, and no sensitive or  
 963           private information is used. As such, no additional safeguards beyond responsible reporting  
 964           and licensing compliance are necessary.

965           Guidelines:

- 966           • The answer NA means that the paper poses no such risks.

- 967           • Released models that have a high risk for misuse or dual-use should be released with  
 968            necessary safeguards to allow for controlled use of the model, for example by requiring  
 969            that users adhere to usage guidelines or restrictions to access the model or implementing  
 970            safety filters.  
 971           • Datasets that have been scraped from the Internet could pose safety risks. The authors  
 972            should describe how they avoided releasing unsafe images.  
 973           • We recognize that providing effective safeguards is challenging, and many papers do  
 974            not require this, but we encourage authors to take this into account and make a best  
 975            faith effort.

976       **12. Licenses for existing assets**

977       Question: Are the creators or original owners of assets (e.g., code, data, models), used in  
 978       the paper, properly credited and are the license and terms of use explicitly mentioned and  
 979       properly respected?

980       Answer: [Yes]

981       Justification: All external assets used in the paper are properly credited and their licenses  
 982       respected. We clearly state that the daily financial data are sourced from CRSP and the  
 983       high-frequency intraday data are obtained from Polygon.io, both under institutional licensing  
 984       agreements. We also acknowledge that these datasets cannot be publicly redistributed due to  
 985       licensing restrictions. Any public libraries or frameworks used for model development and  
 986       training (such as standard deep learning libraries) are cited where appropriate.

987       Guidelines:

- 988           • The answer NA means that the paper does not use existing assets.
- 989           • The authors should cite the original paper that produced the code package or dataset.
- 990           • The authors should state which version of the asset is used and, if possible, include a  
 991            URL.
- 992           • The name of the license (e.g., CC-BY 4.0) should be included for each asset.
- 993           • For scraped data from a particular source (e.g., website), the copyright and terms of  
 994            service of that source should be provided.
- 995           • If assets are released, the license, copyright information, and terms of use in the  
 996            package should be provided. For popular datasets, [paperswithcode.com/datasets](https://paperswithcode.com/datasets)  
 997            has curated licenses for some datasets. Their licensing guide can help determine the  
 998            license of a dataset.
- 999           • For existing datasets that are re-packaged, both the original license and the license of  
 1000            the derived asset (if it has changed) should be provided.
- 1001           • If this information is not available online, the authors are encouraged to reach out to  
 1002            the asset's creators.

1003       **13. New Assets**

1004       Question: Are new assets introduced in the paper well documented and is the documentation  
 1005       provided alongside the assets?

1006       Answer: [Yes]

1007       Justification: The primary new asset introduced in the paper is the implementation code  
 1008       for our statistical arbitrage framework based on rank-space modeling. We provide detailed  
 1009       pseudocode in the Appendix and release the full Python code with accompanying documen-  
 1010       tation and instructions on a public GitHub repository. This ensures that others can faithfully  
 1011       reproduce the main results and understand the implementation details.

1012       Guidelines:

- 1013           • The answer NA means that the paper does not release new assets.
- 1014           • Researchers should communicate the details of the dataset/code/model as part of their  
 1015            submissions via structured templates. This includes details about training, license,  
 1016            limitations, etc.
- 1017           • The paper should discuss whether and how consent was obtained from people whose  
 1018            asset is used.

- 1019           • At submission time, remember to anonymize your assets (if applicable). You can either  
1020           create an anonymized URL or include an anonymized zip file.

1021 **14. Crowdsourcing and Research with Human Subjects**

1022 Question: For crowdsourcing experiments and research with human subjects, does the paper  
1023 include the full text of instructions given to participants and screenshots, if applicable, as  
1024 well as details about compensation (if any)?

1025 Answer: [NA]

1026 Justification: Our research does not involve any crowdsourcing experiments, human subjects,  
1027 or participant studies. All experiments are conducted on historical financial market data  
1028 without human interaction.

1029 Guidelines:

- 1030           • The answer NA means that the paper does not involve crowdsourcing nor research with  
1031           human subjects.  
1032           • Including this information in the supplemental material is fine, but if the main contribu-  
1033           tion of the paper involves human subjects, then as much detail as possible should be  
1034           included in the main paper.  
1035           • According to the NeurIPS Code of Ethics, workers involved in data collection, curation,  
1036           or other labor should be paid at least the minimum wage in the country of the data  
1037           collector.

1038 **15. Institutional Review Board (IRB) Approvals or Equivalent for Research with Human  
1039 Subjects**

1040 Question: Does the paper describe potential risks incurred by study participants, whether  
1041 such risks were disclosed to the subjects, and whether Institutional Review Board (IRB)  
1042 approvals (or an equivalent approval/review based on the requirements of your country or  
1043 institution) were obtained?

1044 Answer: [NA]

1045 Justification: Our research does not involve any study participants or human subjects.  
1046 Therefore, no risks to participants exist, no disclosures were necessary, and no Institutional  
1047 Review Board (IRB) approvals were required.

1048 Guidelines:

- 1049           • The answer NA means that the paper does not involve crowdsourcing nor research with  
1050           human subjects.  
1051           • Depending on the country in which research is conducted, IRB approval (or equivalent)  
1052           may be required for any human subjects research. If you obtained IRB approval, you  
1053           should clearly state this in the paper.  
1054           • We recognize that the procedures for this may vary significantly between institutions  
1055           and locations, and we expect authors to adhere to the NeurIPS Code of Ethics and the  
1056           guidelines for their institution.  
1057           • For initial submissions, do not include any information that would break anonymity (if  
1058           applicable), such as the institution conducting the review.